CANADIAN LIGHT SOURCE INC.

RESEARCH REPORT 2019

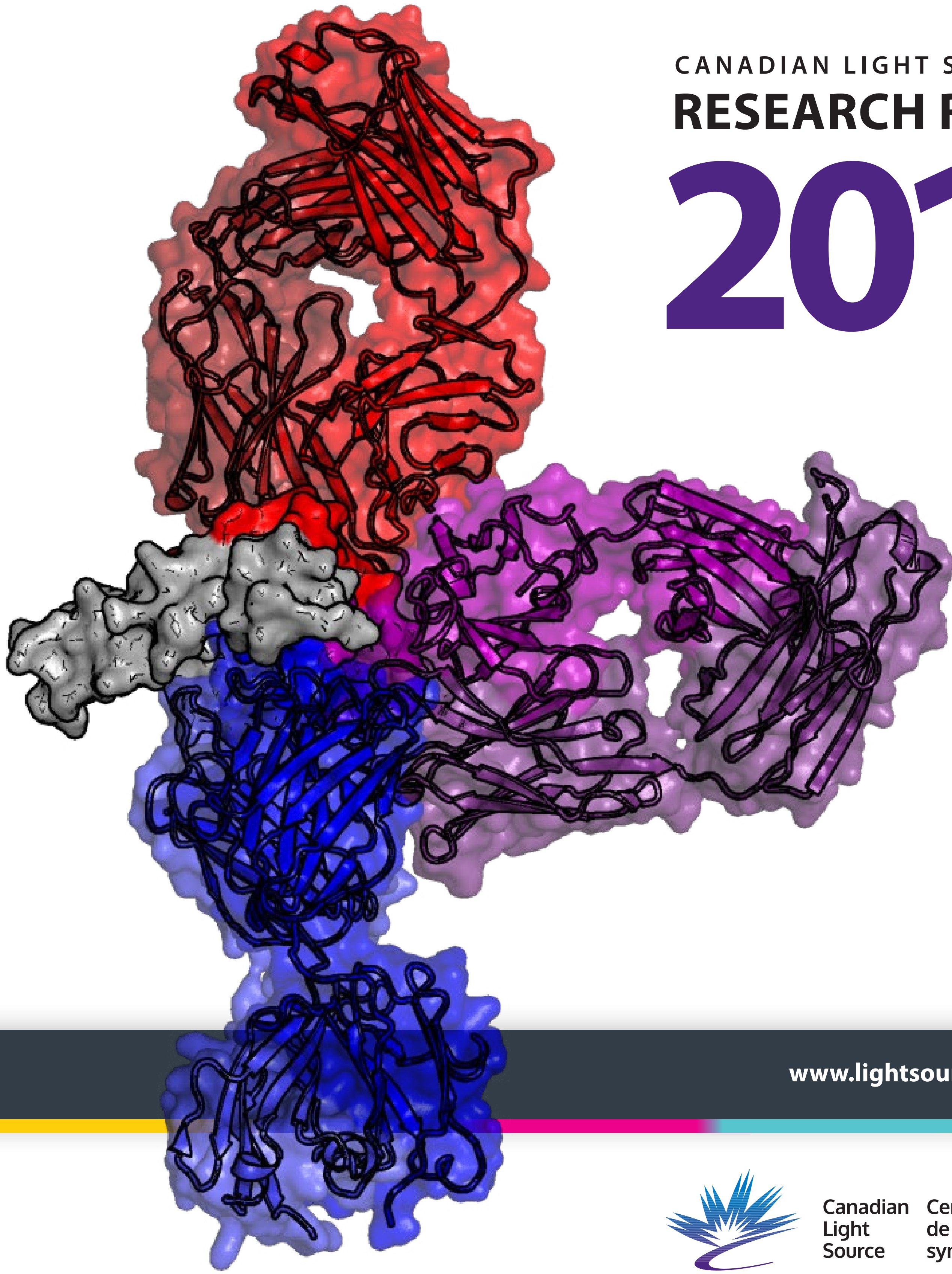

www.lightsource.ca

Canadian Light Source
Centre canadien de rayonnement synchrotron

THE BRIGHTEST LIGHT IN CANADA™

ACKNOWLEDGEMENTS

FUNDING PARTNERS

The Canadian Light Source thanks all of our funding partners for their commitment to the advancement of science and innovation.

OPERATING

CAPITAL

USER INSTITUTIONS

Agriculture and Agri-Food Canada (AAFC)
Aquanty
Aston University
Autonomous University of Chiapas
Benemeritus Autonomous University of Puebla (BUAP)
Ben-Gurion University of the Negev
California State University, Fresno
Canadian Conservation Institute
Center for High Pressure Science & Technology Advanced Research (HPSTAR)
Centre National de la Recherche Scientifique (CNRS)
China Agricultural University
Chinese Academy of Agricultural Science
Chinese Academy of Sciences
Columbia University
Commissariat à l'Energie Atomique, Marcoule
Commissariat à l'Energie Atomique, Saclay
Concordia University
Cornell University
Dalhousie University
Durham University
Environment and Climate Change Canada
Forschungszentrum Jülich
FTXT Energy Technology Co., Ltd.
Fudan University
Global Institute for Food Security
Hanyang University
Harvard Medical School
Helix Biostructures LLC
Helmholtz Institute Ulm
IBM T.J. Watson Research Center
Institut National de la Recherche Scientifique
Institute for Energy, Environment and Sustainable Communities
Institute of Applied Ecology
Institute of Environmental and Sustainable Development in Agriculture
Iona College
Iwate University
James Madison University
Kansas State University
Kent State University
Korea Research Institute of Standards and Science
Lamar University
Lanzhou University
Laurentian University
Lawrence Berkeley National Laboratory
Lawrence Livermore National Laboratory
Leibniz Institute for Solid State Physics and Materials Research Dresden (IFW Dresden)
Lund University
Massachusetts Institute of Technology
Max Planck Institute for Chemical Physics of Solids
Mayo Clinic
McGill University
McMaster University
Memorial University of Newfoundland
Montana State University
Mount Allison University
National Institute of Standards and Technology
National Research Council of Canada
Natural Resources Canada
Oak Ridge National Laboratory
Ohio State University
Oklahoma State University
Old Dominion University
Pacific Northwest National Laboratory
Peking University
Programa Multidisciplinario de Posgrado en Ciencias Ambientales UASLP
Purdue University
Qingdao University
Queen's University
Royal Saskatchewan Museum
Royal Tyrrell Museum
Saskatchewan Polytechnic
Savannah River National Laboratory
Seoul National University
Shanghai Institute of Applied Physics
ShanghaiTech University
Simon Fraser University
SLAC National Accelerator Laboratory
Smithsonian Astrophysical Observatory
Soochow University
Sookmyung Women's University
Southwest Petroleum University
Stanford Synchrotron Radiation Lightsource
Stanford University
State University of New York, Buffalo
Texas A and M University
The Hospital for Sick Children
TR Labs
Trinity College, Dublin
Trinity University
Tulane University
UChicago Argonne LLC
Université de Montréal
Université du Québec à Montréal
Université Laval
Universiteit Twente
University Medical Center Goettingen, Germany
University of Akron
University of Alberta
University of Antwerp
University of Arizona
University of Bayreuth
University of Bristol
University of British Columbia
University of Calgary
University of California, Davis
University of California, Merced
University of California, Riverside
University of Cambridge
University of Colorado Boulder
University of Connecticut
University of Delaware
University of Guelph
University of Idaho
University of Illinois at Urbana–Champaign
University of Kansas
University of Lethbridge
University of Manitoba
University of Maryland Baltimore County
University of Massachusetts
University of Minnesota
University of Nebraska
University of Nevada, Las Vegas
University of New Brunswick
University of North Carolina at Chapel Hill
University of Northern British Columbia
University of Ottawa
University of Oulu
University of Pennsylvania
University of Regina
University of Rostock
University of Saskatchewan
University of South Australia
University of Tasmania
University of Tennessee
University of Texas, Arlington
University of the Pacific
University of Toronto
University of Vermont
University of Victoria
University of Waterloo
University of Western Ontario
University of Windsor
University of Winnipeg
University of Wuppertal
University of Wyoming
Virginia Polytechnic and State University
Washington State University
Wilfrid Laurier University
Yale University
York University
Zhejiang University

TABLE OF CONTENTS

Canadian Light Source Research Report 2019
Editor: Victoria Martinez

www.lightsource.ca

Layout and cover design: Reach Communications

Cover: Protein structure of Pfs25 and bound antibodies captured at CMCF. See page 4.

SCIENCE DIRECTOR'S MESSAGE

This is my first message as Science Director of the CLS and I want to convey my experience one year into my appointment. I have been impressed by the dedication, perseverance and efforts of the entire CLS staff as well as the support and encouragement I have received since I joined the CLS team. Coming from a different academic and research environment I appreciate the cooperation, professionalism and team efforts of the entire CLS staff. No wonder that the science output from this team is so impressive and impactful. This past year, as always, the CLS has produced enormously diverse research supporting the equally diverse user base in Canada and beyond.

Indeed, this report highlights some of the most exciting research in health, agriculture, energy and the environment, and advanced materials from the last year. In health, we see new work on converting donated blood to a universal blood type. In agriculture, researchers have been working on new approaches for nutrient analysis of vital food crops. Materials researchers have made great strides in electrocatalytic conversion of greenhouse gases to useful products, such as engine fuel. And environmental researchers are pushing our understanding of the carbon cycle in our soils.

Our research community continues to grow and thrive. We closed 2019 with a record number of proposals for the January-June 2020 cycle, a record we hope to build on in coming years. With all of our Phase III beamlines – BioXAS, QMSC and BXDS – now in scientific commissioning and demonstrating outstanding results, we will build on the already strong collaborations we have with universities, government and industry, and the exciting new avenues of inquiry these beamlines will enable.

This was a landmark year for our burgeoning agricultural science program. The CLS was the first synchrotron to define agricultural science as one of its strategic priorities, due to the combination of its unique capabilities, in-house expertise, and close proximity to outstanding agricultural science infrastructure. In addition to the research published on soils, plant diseases and plant breeding, we hosted the first international Pan-American Light Sources for Agriculture (PALSA) conference, showcasing the value of light sources for agricultural research and connecting a growing global research community.

Our educational programming continues to reach new audiences, bringing synchrotron science to curious young minds across Canada. In partnership with the University of Saskatchewan's Mistik Askiwin Dendrochronology Laboratory (MAD Lab), the new Trans-Canadian Research and Environmental Education (TREE) program combines CLS techniques for chemical analysis and MAD Lab expertise in the science of tree rings, to paint a detailed picture of how trembling aspen are doing in communities throughout Canada.

2019 was also an important year for looking to the future of Canadian synchrotron science, as our accelerator physicists developed preliminary designs for CLS 2.0, the next facility to serve our strong research community. We are also working with the Canadian synchrotron user community to develop the plans that will maintain our global competitiveness in synchrotron science.

We ended the fiscal year on a darker note, with the global COVID-19 crisis that has affected every corner of the world. As I write this, after being dark for several weeks to protect our staff and users, the CLS is restarting operations to bring the light back to help the research community to fight the war against this virus. We also had a successful special call for proposals for COVID-19 related research with users across Canada responding. For me, this special call is very symbolic for everyone at CLS, Canada needs to have the light shine again. We want to be part of the global war against this virus and our role is to use our beamlines to know more about our enemy.

Finally, I extend our gratitude to our funding partners for continuing to support our operations and the world-caliber science of the over 1,000 Canadian scientists that use CLS every year. Thank you.

Gianluigi Botton
Science Director

Throughout this report, the following symbols will be used to indicate the techniques of highlighted research.

IMAGING **SPECTROSCOPY** **DIFFRACTION**

HEALTH

Nebulized hypertonic saline triggers nervous system-mediated active liquid secretion in cystic fibrosis swine trachea

Xiaojie Luan, Julian S. Tam, George Belev, Santosh Jagadeeshan, Brendan Murray, Noman Hassan, Terry E. Machen, L. Dean Chapman & Juan P. Ianowski

BMIT

Inhaled hypertonic saline (HTS) treatment is used to improve lung health in patients with cystic fibrosis (CF). The current consensus is that the treatment generates an osmotic gradient that draws water into the airways and increases airway surface liquid (ASL) volume. However, there is evidence that HTS may also stimulate active secretion of ASL by airway epithelia through the activation of sensory neurons. The researchers tested the contribution of the nervous system and airway epithelia on HTS-stimulated ASL height increase in CF and wild-type swine airway. We used synchrotron-based imaging to investigate whether airway neurons and epithelia are involved in HTS treatment-triggered ASL secretion in CFTR–/– and wild-type swine. We showed that blocking parasympathetic and sensory neurons in airway resulted in ~50% reduction of the effect of HTS treatment on ASL volume in vivo. Incubating tracheal preparations with inhibitors of epithelial ion transport across airway decreased secretory responses to HTS treatment. CFTR–/– swine ex-vivo tracheal preparations showed substantially decreased secretory response to HTS treatment after blockage of neuronal activity. Our results indicated that HTS-triggered ASL secretion is partially mediated by the stimulation of airway neurons and the subsequent activation of active epithelia secretion; osmosis accounts for only ~50% of the effect.

Cystic fibrosis is one of the most common fatal genetic diseases affecting Canadian children and young adults. This study shows that inhaled hypertonic saline treatment stimulates the nervous system, which in turn triggers airway surface liquid secretion.

https://doi.org/10.1038/s41598-018-36695-4

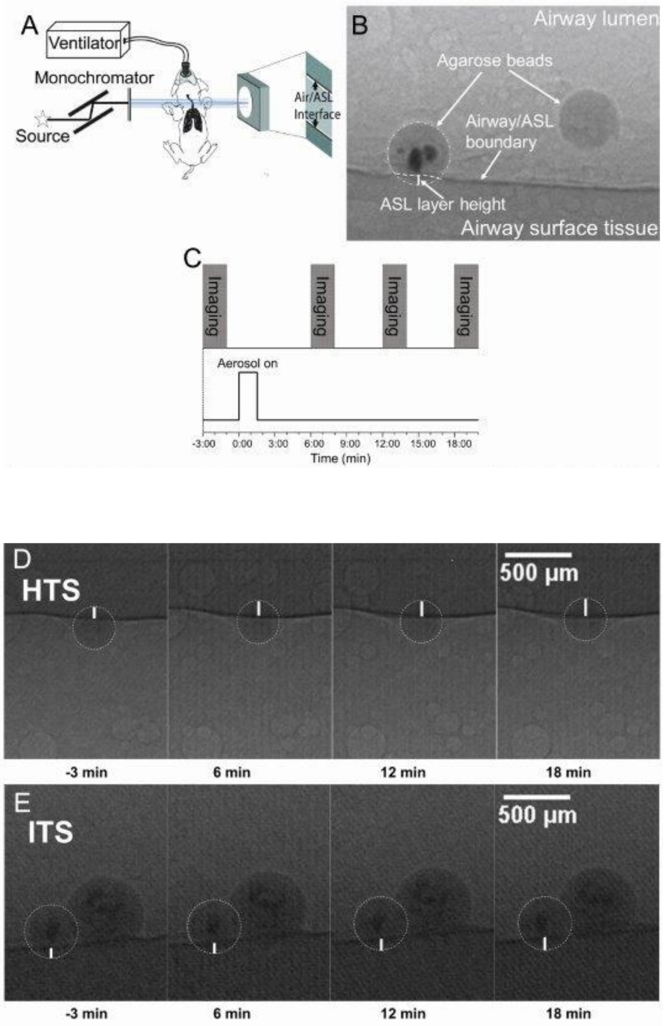

Experimental design and phase contrast imaging using synchrotron X-rays. (A) Schematic showing the set-up for ASL height measurement in the lumen of the trachea using phase contrast imaging. When X-rays pass through the preparation, the difference in refractive index between the ASL and the air results in a phase shift of X-rays that causes a distinct interference pattern detected as variations in X-ray intensities on the charge-coupled device detector. (B) Synchrotron-based phase contrast imaging measurement of ASL height in an isolated swine trachea. (C) HTS or isotonic saline (ITS) aerosol were delivered at time 0 for 90 seconds, and images were acquired at time −3, 6, 12, and 18 minutes. Representative sample of the images acquired from an ex vivo preparation treated with (D) HTS and (E) ITS nebulization at −3, 6, 12, and 18 minutes.

An enzymatic pathway in the human gut microbiome that converts A to universal O type blood

Peter Rahfeld, Lyann Sim, Haisle Moon, Iren Constantinescu, Connor Morgan-Lang, Steven J. Hallam, Jayachandran N. Kizhakkedathu & Stephen G. Withers

CMCF

Half of all Canadians will either need blood or know someone who needs it in their lifetime. This work describes a mechanism whereby A and B type red blood cells can be converted to universal-donor O type, which would greatly increase the supply of blood for transfusions.

Access to efficient enzymes that can convert A and B type red blood cells to 'universal' donor O would greatly increase the supply of blood for transfusions. Here we report the functional metagenomic screening of the human gut microbiome for enzymes that can remove the cognate A and B type sugar antigens. Among the genes encoded in our library of 19,500 expressed fosmids bearing gut bacterial DNA, we identify an enzyme pair from the obligate anaerobe Flavonifractor plautii that work in concert to efficiently convert the A antigen to the H antigen of O type blood, via a galactosamine intermediate. The X-ray structure of the N-acetylgalactosamine deacetylase reveals the active site and mechanism of the founding member of an esterase family. The galactosaminidase expands activities within the CAZy family GH36. Their ability to completely convert A to O of the same rhesus type at very low enzyme concentrations in whole blood will simplify their incorporation into blood transfusion practice, broadening blood supply.

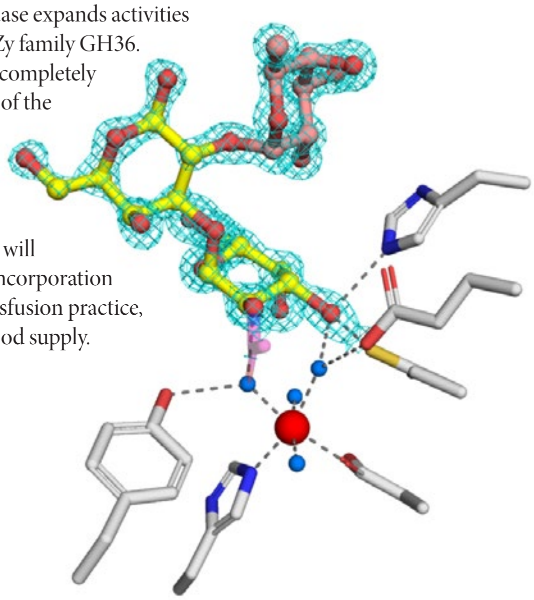

Active site of the GalNAc deacetylase enzyme with a substrate analogue bound

https://doi.org/10.1038/s41564-019-0469-7

Cross-linked elastin-like polypeptide membranes as a model for medial arterial calcification

Ophélie Gourgas, Lisa D. Muiznieks, Dainelys Guadarrama Bello, Antonio Nanci, Simon Sharpe, Marta Cerruti

SXRMB

This paper presents a simplified laboratory model that mimics the formation of the mineral deposits that harden arteries and lead to several adverse outcomes including heart attacks and strokes.

Calcium phosphate minerals deposit on the elastin-rich medial layers of arteries in the majority of seniors, diabetic, and chronic kidney disease patients, causing severe cardiovascular complications. There is no cure for medial calcification, and the mechanism of mineral formation on elastin layers is unknown. Here we propose cross-linked elastin-like polypeptide membranes as models to study medial calcification. Calcium phosphates deposit first on fibers and filaments and then spread to globular structures present in the membranes. Mineral phase evolution analyzed by near-edge X-ray spectroscopy matches that previously observed in a mouse model of medial calcification, showing that this simple system captures some of the key in vivo findings. This work shows how minerals form and evolve upon nucleation on elastin and provides an in vitro model that can be tuned to study hypotheses related to arterial calcification mechanisms and test drugs to stop or revert mineralization.

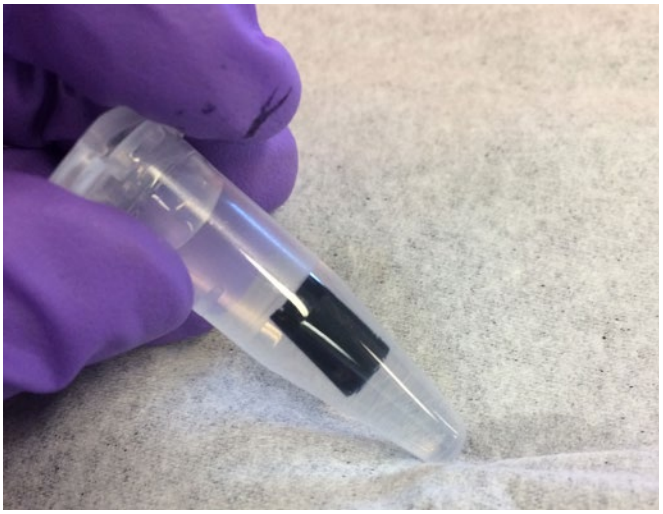

A membrane made of elastin-like peptide immersed in simulated body fluids. The blue color is due to the crosslinker, genipin.

https://doi.org/10.1021/acs.biomac.9b00417

Potent antibody lineage against malaria transmission elicited by human vaccination with Pfs25

Brandon McLeod, Kazutoyo Miura, Stephen W. Scally, Alexandre Bosch, Ngan Nguyen, Hanjun Shin, Dongkyoon Kim, Wayne Volkmuth, Sebastian Rämisch, Jessica A. Chichester, Stephen Streatfield, Colleen Woods, William R. Schief, Daniel Emerling, C. Richter King & Jean-Philippe Julien

CMCF

Transmission-blocking vaccines have the potential to be key contributors to malaria elimination. Such vaccines elicit antibodies that inhibit parasites during their development in Anopheles mosquitoes, thus breaking the cycle of transmission. To date, characterization of humoral responses to Plasmodium falciparum transmission-blocking vaccine candidate Pfs25 has largely been conducted in pre-clinical models. Here, we present molecular analyses of human antibody responses generated in a clinical trial evaluating Pfs25 vaccination. From a collection of monoclonal antibodies with transmission-blocking activity, we identify the most potent transmission-blocking antibody yet described against Pfs25; 2544. The interactions of 2544 and three other antibodies with Pfs25 are analyzed by crystallography to understand structural requirements for elicitation of human transmission-blocking responses. Our analyses provide insights into Pfs25 immunogenicity and epitope potency, and detail an affinity maturation pathway for a potent transmission-blocking antibody in humans. Our findings can be employed to guide the design of improved malaria transmission-blocking vaccines.

https://doi.org/10.1038/s41467-019-11980-6

In 2017 alone, there were an estimated 219 million malaria cases, leading to approximately 435,000 deaths worldwide. This paper provides the first detailed molecular analysis of the structures of a candidate transmission-blocking vaccine.

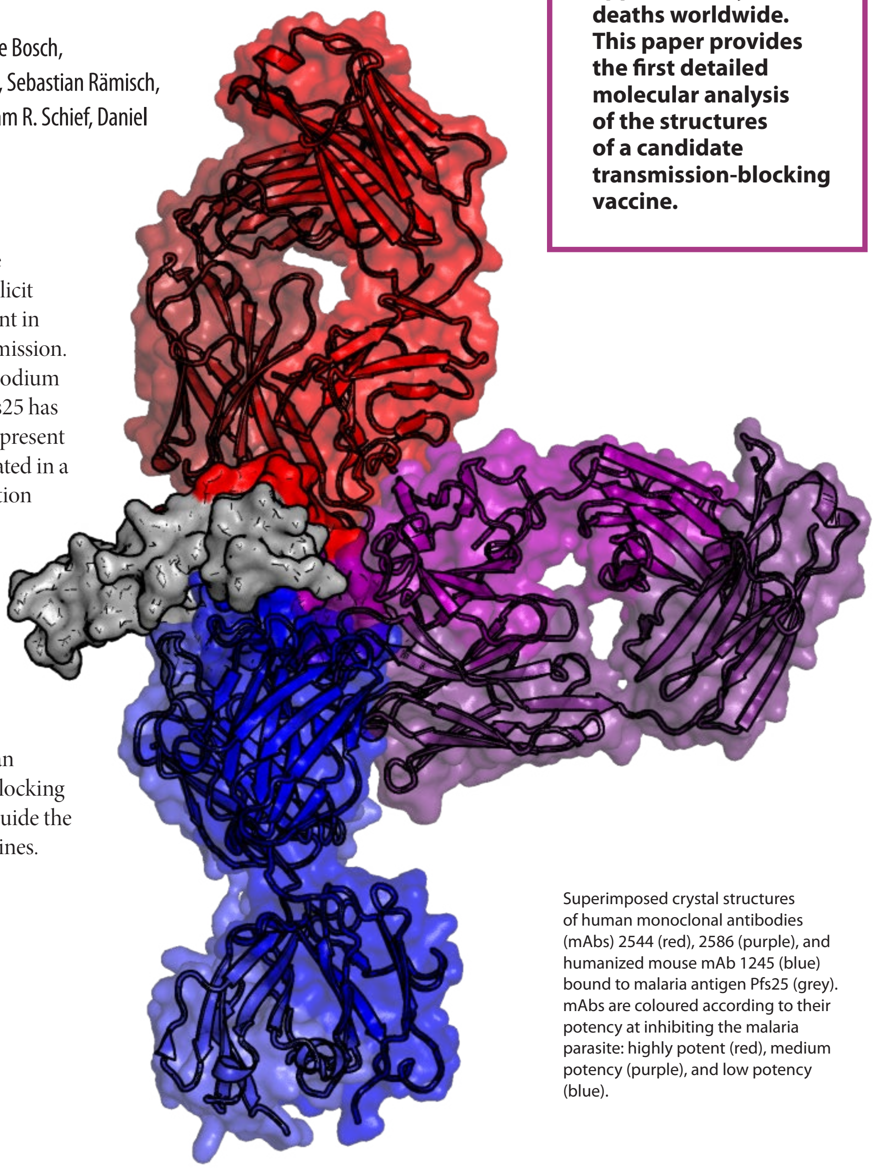

Superimposed crystal structures of human monoclonal antibodies (mAbs) 2544 (red), 2586 (purple), and humanized mouse mAb 1245 (blue) bound to malaria antigen Pfs25 (grey). mAbs are coloured according to their potency at inhibiting the malaria parasite: highly potent (red), medium potency (purple), and low potency (blue).

AGRICULTURE

A look into the past: Tracing ancient sustainable manuring practices by thorough P speciation of northern European anthrosols

Andre Acksel, Karen Baumann, Yongfeng Hu, Peter Leinweber

SXRMB

Analysis of soil samples from 12 sites in Germany, Norway and Denmark, with uniquely long-lasting fertility. Soil profiles indicated ancient applications of peat, animal manure, composts and biochar.

Regionally restricted, humus-rich topsoils in Southwest Norway and the Baltic Sea region of Germany and Denmark were formed by inputs of various amendments (combustion residues and marine biomass) and, therefore, were classified as Anthrosols. For a deeper insight into the ancient management practices, we investigated the elemental and P-composition in the upper and underlying horizons from 12 soil profiles in the Jæren region, at the islands of Karmøy and Feøy (Norway), at the island of Fehmarn and the peninsula of Wagrien (Germany), and at the islands of Poel (Germany) and Sjaelland (Denmark). We used aqua regia digestion and the complementary methods of sequential P fractionation, phosphorus K-edge X-ray absorption near edge structure (P-XANES) spectroscopy, and ^{31}P nuclear magnetic resonance (^{31}P-NMR) spectroscopy. Results were compared with the composition of differently amended and/or un-amended soils from other studies. In addition, archaeological literature was used to confirm possible inputs of specific P-containing amendments in ancient agriculture. The P composition from SF of the Anthrosols in Norway (44% NaOH-P_i > 18% NaOH-Po > 14% $NaHCO_3$-P_i, 12% H_2SO_4-P > 7% $NaHCO_3$-Po > 3% residual-P = 3% resin-P) and complementary archaeological literature provided strong indication for the use of peat, sheep manure, compost, and human excreta. The Anthrosols in the Jæren region have been formed from peat, which had been used as alternative bedding material and had been mixed with sheep and/or cattle manure. The P-composition in the Anthrosols at the island of Fehmarn and at the peninsula of Wagrien (42% H_2SO_4-P > 25% residual-P > 10% NaOH-P_o, 8% NaOH-P_i: > 6% $NaHCO_3$-P_i and $NaHCO_3$-P_o, 4% resin-P) resulted from the application of domestic cattle manure. This was strongly supported by archaeological findings of cattle bones in this region, as well as high proportions of Ca-P, as confirmed by P-XANES. The predominance of Po in the Anthrosols at the island of Poel and Sjaelland (31% NaOH-P_o > 23% NaHCO3-P_o, 21% H_2SO_4-P > 11% NaOH-Pi > 8% $NaHCO_3$-Pi > 4% residual-P, 3% resin-P, in agreement with results from ^{31}P-NMR) indicated low ancient inputs of various excrement or manure. This was supported by low livestock history at the island of Poel. In conclusion, these agricultural techniques can be considered as sustainable P recycling and soil amendment since they improved soil fertility for many generations.

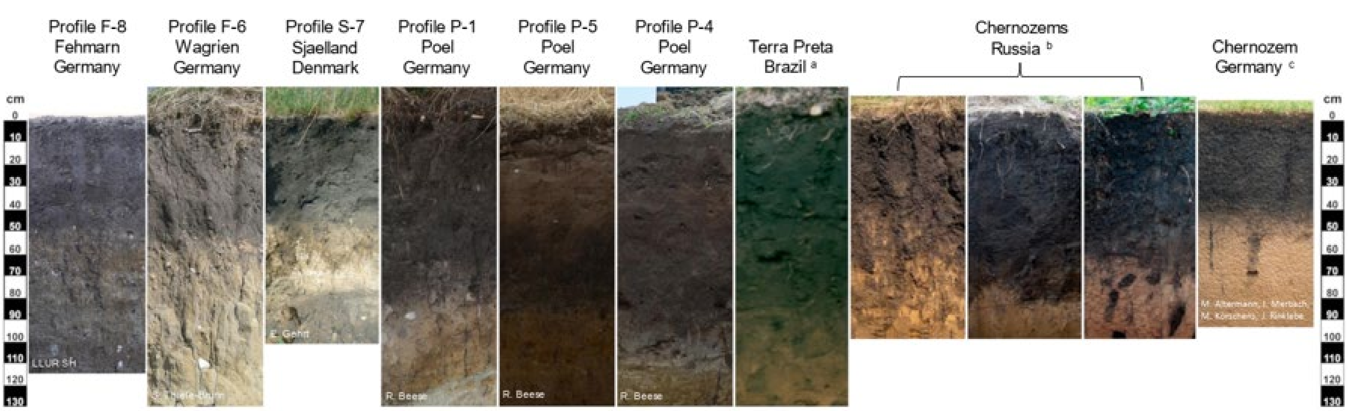

Morphological comparison of the soil profiles of the Northern Europe Anthrosols under this study and various deep, dark humus-rich soils from Europe and Brazil. (a) Glaser et al. (2001); (b) Chendev et al. (2015); (c) dbges.de (2019)

https://doi.org/10.3390/soilsystems3040072

Evaluation of X-Ray fluorescence spectroscopy as a tool for nutrient analysis of pea seeds

Pea proteins are the main ingredient in protein based meat alternative foods, which is one reason that undertanding the nutritional profiles of the legumes is commercially important. This work is a proof-of-concept for X-ray fluorescence as a nutrient profiling technique.

Ramandeep K. Bamraha, Perumal Vijayana, Chithra Karunakaran, David Muir, Emil Hallin, Jarvis Stobbs, Barry Goetz, Michael Nickerson, Karen Tanino and Thomas D. Warkentin

IDEAS

This research was conducted to evaluate the utility and reliability of X-ray fluorescence (XRF) spectroscopy to analyze macro- (K and Ca) and micronutrients (Mn, Fe, Cu, Zn, and Se) in pea (*Pisum sativum* L.) seeds. The pea seed samples were ground into flour and pelleted to collect the XRF spectra. 73 pea seed samples were selected to cover the expected concentration ranges for each element to develop calibration curves by correlating the XRF results with atomic absorption spectroscopy (AAS). The XRF results were validated by a systematic comparison of data obtained from AAS on a set of 80 additional and independent pea seed samples. Element concentrations were also predicted using the fundamental parameter approach collectively for 153 samples. For all the calibration curves, the R^2 value was >0.8, except for K (0.54). For Mn, Fe, Cu, Zn, and Se, the XRF predictions were similar to AAS measurements at a 95% confidence level. Similar results were obtained with the fundamental parameter approach except for Fe for which significant bias of ~6 mg kg_{-1} was calculated. Except for K, R value for all the validation curves was >0.85. Thus, the results obtained using XRF and the fundamental parameter approach were statistically not different from the AAS method. This study demonstrated that the XRF technique is a fast and reliable, nondestructive, and noninvasive analytical tool for mineral analysis, particularly for transition metals, does not produce waste, and requires no chemical reagents.

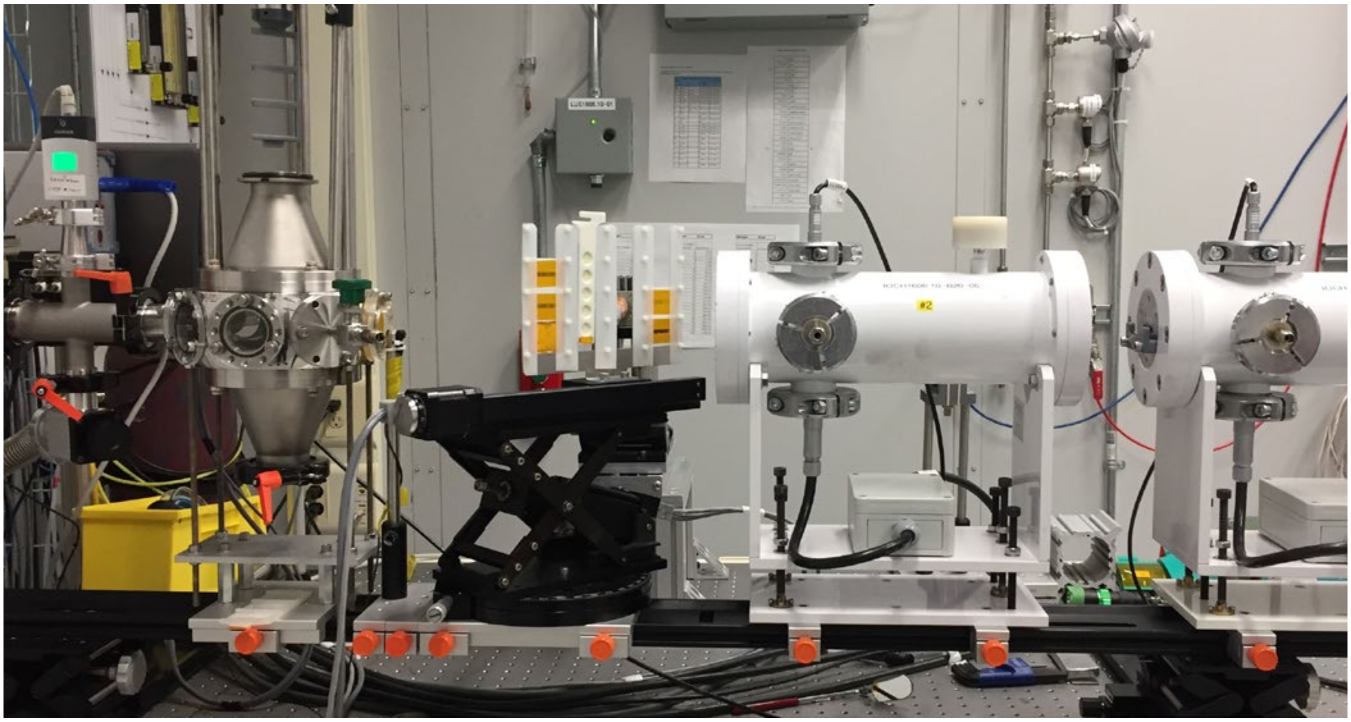

Instrument set up for XRF pea analysis.

https://doi.org/10.2135/cropsci2019.01.0004

High throughput nutritional profiling of pea seeds using Fourier transform mid-infrared spectroscopy

Chithra Karunakaran, Perumal Vijayan, Jarvis Stobbs Ramandeep Kaur Bamrah, Gene Arganosa, Thomas D. Warkentin

Mid-IR

Presents the development of a fast and cost-effective method for nutritional profiling of pea seeds using Fourier transform mid-infrared spectroscopy.

Seed samples from 117 genetically diverse pea breeding lines were used to determine the robustness of Fourier transform mid-infrared spectroscopy (FT-MIR) for the rapid nutritional profiling of seeds. The FT-MIR results were compared to wet chemistry methods for assessing the concentrations of total protein, starch, fiber, phytic acid, and carotenoids in pea seed samples. Of the five partial least square regression models (PLSR) developed, protein, fiber and phytic acid concentrations predicted by the models exhibited correlation coefficients greater than 0.83 when compared with data obtained using the wet chemistry methods for both the calibration and validation sets. The starch PLSR model had a correlation greater than 0.75, and carotenoids had correlation of 0.71 for the validation sets. The methods implemented in this research show the novelty and usefulness of FT-MIR as a simple, fast, and cost-effective technique to determine multiple seed constituents simultaneously.

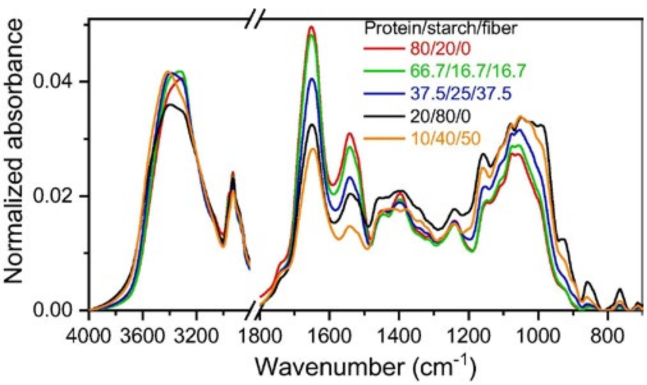

Representative FT-MIR spectra of pea seed fractions at different combinations of protein, starch, and fiber concentrations. Each constituent is expressed as percent weight of the sample used.

https://doi.org/10.1016/j.fochx.2019.100055

The effects of sodium reduction on the gas phase of bread doughs using synchrotron X-ray microtomography

Xinyang Sun, Martin G. Scanlon, Reine-Marie Guillermic, George S. Belev, M. Adam Webb, Serdar Aritan, Michael T. Nickerson, Filiz Koksel

BMIT

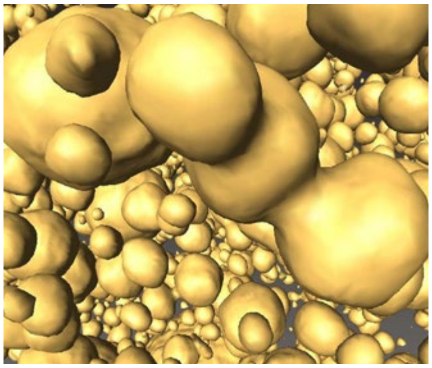

Bread dough as seen using BMIT. A dough sample of approximately 83mm^3 contains over 24,000 bubbles.

Globally, the bakery industry has a target of reducing sodium content in bread products. However, removing salt results in changes in the quality of bread through effects on dough's gas phase during the breadmaking process. Using synchrotron X-ray microtomography, the objective of this study was to investigate how sodium reduction induced changes in the gas phase parameters (i.e., gas volume fraction, bubble size distribution (BSD) and its time evolution) of non-yeasted doughs made from a wide range of formulations (i.e., wheat cultivar and water content) prepared with different mixing times. As salt content was reduced, a lower gas volume was retained in the dough by the end of mixing. Less gas bubbles were also retained if doughs were prepared from a stronger wheat cultivar, higher water content, and/or mixed for a shorter time. Rates of change in the median (R_0) and the width (ε) of the fitted lognormal radius dependence of bubble volume fraction [BVF(R)] indicated that reduced sodium content permitted disproportionation to proceed more rapidly. Higher water content or longer mixing time also resulted in faster disproportionation, indicating that water content and mixing time can be manipulated as a means of increasing bubble stability against disproportionation during low-sodium breadmaking. An examination of relative changes in dough's gas phase parameters arising from sodium reduction demonstrated that wheat cultivar, water content and mixing time all affected dough's tolerance to sodium reduction. Therefore, attainment of good bread crumb cell structure in low-sodium bread formulas is a function of salt's effects on dough rheology in addition to its effect on yeast activity, so that dough formulation and mixing conditions also need to be considered.

Study of simple non-yeast doughs to assess how varying the salt content affects bubble formation and dough-handling properties. Reduced sodium breads could help Canadians meet Health Canada recommendations to reduce dietary sodium intake.

https://doi.org/10.1016/j.foodres.2019.108919

ENVIRONMENT

Effects of bio-additives on the physicochemical properties and mechanical behavior of canola hull fuel pellets

Ramin Azargohar, Sonil Nanda, Kang Kang, Toby Bond, Chithra Karunakaran, Ajay K. Dalai, Janusz A. Kozinski

BMIT

Agricultural residues can be converted to value-added products such as fuel pellets. Bio-based additives, including alkali lignin, glycerol and l-proline were used for binding formulation of canola hull fuel pellets. The binding formulation was optimized to produce pellet with the mechanical durability (by drop test) of 99%, relaxed density of 1,110 kg/m^3, and energy density of 18,603 MJ/m^3. l-proline showed the best performance in the enhancement of mechanical properties of pellet when compared with other two amino acids. Comparing with pure glycerol, use of crude glycerol decreased compression energy required for pelletization, but resultant pellet had lower tensile strength. SEM and light microscopy showed the effects of lacking moisture, lignin and l-proline in the formulation. Synchrotron-based computed tomography was used for 3D imaging of fuel pellets yielding estimated porosity values over a range of 1.3–5.7% for different fuel pellets. The effects of pelletization operating conditions were also investigated on the pellets.

Canola is one of the most important oilseed crops in Canada and worldwide. Learning how to efficiently recycle byproducts of production into fuel is very important for our environment.

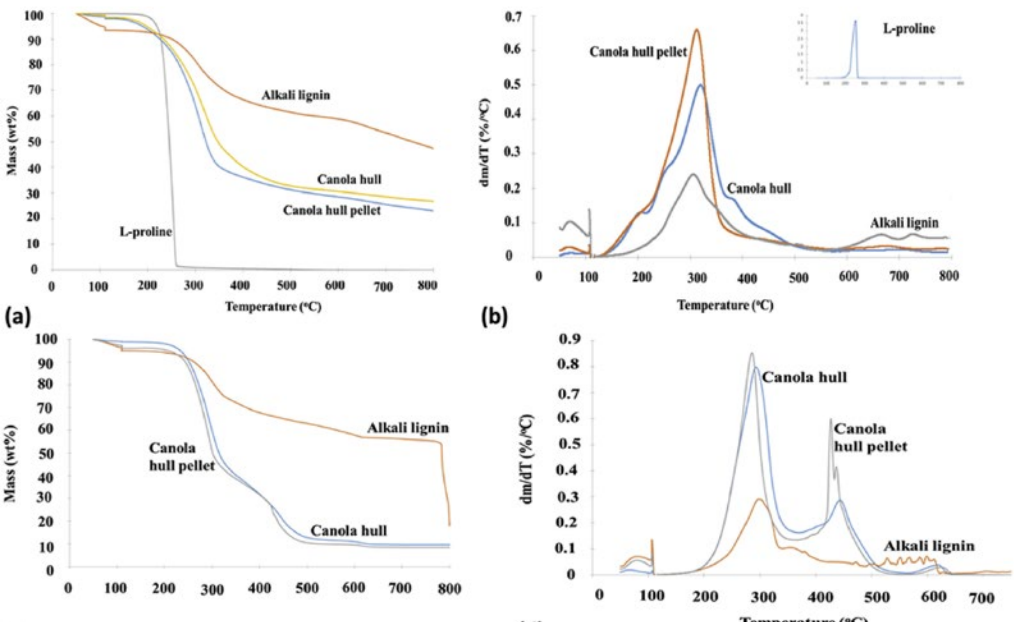

https://doi.org/10.1016/j.renene.2018.08.003

A method for redox mapping by confocal micro-X-ray Fluorescence Imaging: Using chromium species in a biochar particle as an example

Peng Liu, Carol J. Ptacek, David W. Blowes, Y. Zou Finfrock, Mark Steinepreis, Filip Budimir

Agricultural residues can be converted to value-added products such as fuel pellets. Bio-based additives, including alkali lignin, glycerol and l-proline were used for binding formulation of canola hull fuel pellets.

CLS@APS

Redox mapping of solid-phase particles has been used for speciation mapping of near-surface materials or within grains through the use of thin-sections without depth information. Here, a procedure is presented for data collection and processing of depth-dependent redox mapping within solid particles using confocal micro-X-ray fluorescence imaging (CMXRFI). The procedure was applied to a biochar particle that was reacted with Cr(VI)-spiked water. The total Cr distribution was first obtained at an above-edge energy of the K-edge, and showed that Cr was primarily distributed near the surface of the particle. Redox mapping was conducted at 33 representative energies and linear combination fitting (LCF) was performed for the 33 data points from each pixel. The results indicate Cr(III) is the primary species with fractions ranging from 0.6 to 1 and that this fraction is greater in the interior pixels of the particle than at the surface; in contrast, the Cr(VI) fraction is greater at the surface than for interior pixels. The results likely indicate Cr(VI) was first adsorbed and diffused into the biochar, and then reduced to Cr(III). With more Cr(VI) adsorption and the exceedance of the reduction potential of the biochar, remaining Cr(VI) was accumulated on the surface. The redox mapping method was validated by micro-X-ray absorption near-edge structure (XANES) and X-ray photoelectron spectroscopy (XPS) results. This demonstration indicates the developed method combined with CMXRFI can be used to delineate the distribution of different oxidation states of an element within an intact particle or layer.

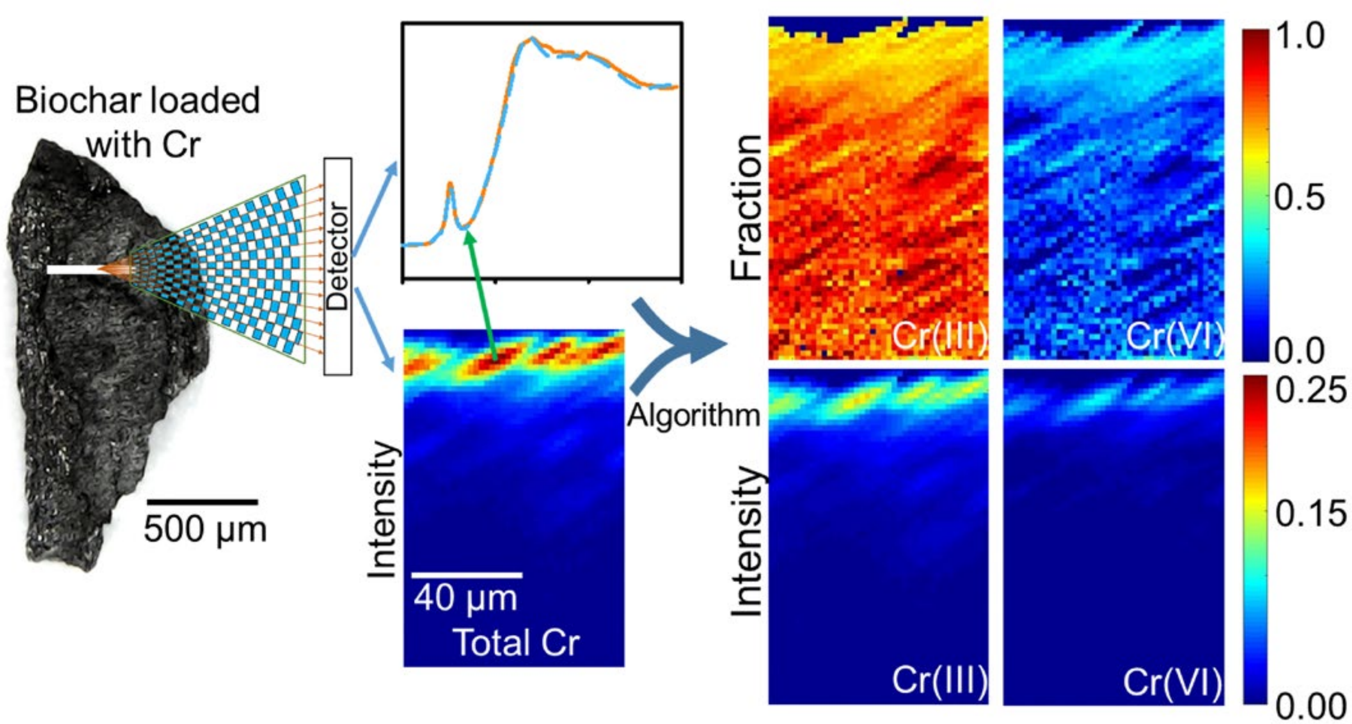

https://doi.org/10.1021/acs.analchem.8b05718

Interactive toxicity of triclosan and nano-TiO_2 to green alga *Eremosphaera viridis* in Lake Erie: A new perspective based on Fourier Transform Infrared Spectromicroscopy and synchrotron-based X-ray Fluorescence Imaging

Xiaying Xin, Gordon Huang, Chunjiang An, Renfei Feng

Triclosan is a common antimicrobial used in soaps and other personal care products, while titanium dioxide is found in many cosmetic products, including sunscreens. Both are of concern in aquatic environments, and this study explores their combined effect on green algae.

VESPERS

This study explored the toxicity of triclosan in the presence of TiO_2 P25 to the green alga *Eremosphaera viridis* in Lake Erie. Multiple physicochemical end points were conducted to perform a comprehensive analysis of the toxic effects of individual and combined pollutants. Fourier transform infrared spectromicroscopy and synchrotron-based X-ray fluorescence imaging were first documented to be applied to explore the distribution variation of macromolecules and microelements in single algal cells in interactive toxicity studies. The results were different based on different triclosan concentrations and measurement end points. Comparing with individual pollutants, the toxicity intensified in lipids, proteins, and oxidative stress at 1000 and 4000 µg/L triclosan in the presence of P25. There were increases in dry weight, chlorophyll content, lipids, and catalase content when cells were exposed to P25 and 15.625 µg/L triclosan. The toxicity alleviated when P25 interacted with 62.5 and 250 µg/L triclosan compared with triclosan-only exposure. The reasons could be attributed to the combination of adsorption, biodegradation, and photocatalysis of triclosan by algae and P25, triclosan dispersion by increased biomass, triclosan adherency on algal exudates, and triclosan adsorption site reduction on algae surface owing to P25's taking over. This work provides new insights into the interactive toxicity of nanoparticles and personal care products to freshwater photosynthetic organisms. The findings can help with risk evaluation for predicting outcomes of exposure to mixtures and with prioritizing further studies on joint toxicity.

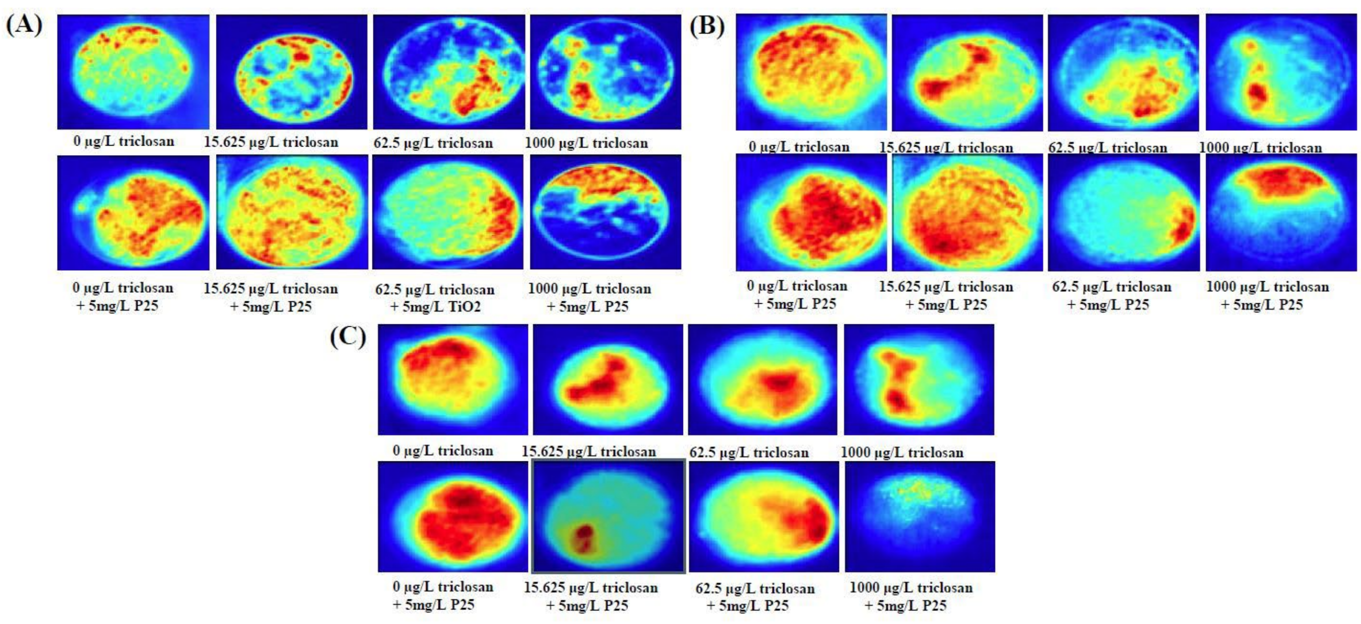

The distribution of major bands for lipids and proteins in an individual algal cell. (A)3000-2800 cm^{-1} C-H stretch in acyl from fatty acids/lipids; (B) ~1740 cm^{-1} C=O in ester and ester fatty acids; (C) 1724-1585 cm^{-1} C=O stretch of Amide I.

https://doi.org/10.1021/acs.est.9b03117

Dissolved organic matter sorption and molecular fractionation by naturally occurring bacteriogenic iron

Tyler D. Sowers, Kathryn L. Holden, Elizabeth K. Coward, Donald L. Sparks

SM

Iron (oxyhydr)oxides are highly reactive, environmentally ubiquitous organic matter (OM) sorbents that act as mediators of terrestrial and aqueous OM cycling. However, current understanding of environmental iron (oxyhydr)oxide affinity for OM is limited primarily to abiogenic oxides. Bacteriogenic iron (oxyhydr)oxides (BIOs), common to quiescent waterways and soil redox transitions, possess a high affinity for oxyanions (i.e., arsenate and chromate) and suggests that BIOs may be similarly reactive for OM. Using adsorption and desorption batch reactions, paired with Fourier transform infrared spectroscopy and Fourier transform ion cyclotron resonance mass spectrometry, this work demonstrates that BIOs are capable of sorbing leaf litter-extracted dissolved organic matter (DOM) and Suwannee River Humic/Fulvic Acid (SRHA/SRFA) and have sorptive preference for distinct organic carbon compound classes at the biomineral interface. BIOs were found to sorb DOM and SRFA to half the extent of 2-line ferrihydrite per mass of sorbent and was resilient to desorption at high ionic strength and in the presence of a competitive ligand. We observed the preferential sorption of aromatic and carboxylic-containing species and concurrent solution enrichment of aliphatic groups unassociated with carboxylic acids. These findings suggest that DOM cycling may be significantly affected by BIOs, which may impact nutrient and contaminant transport in circumneutral environments.

This paper contributes to understanding of organic matter and carbon cycling.

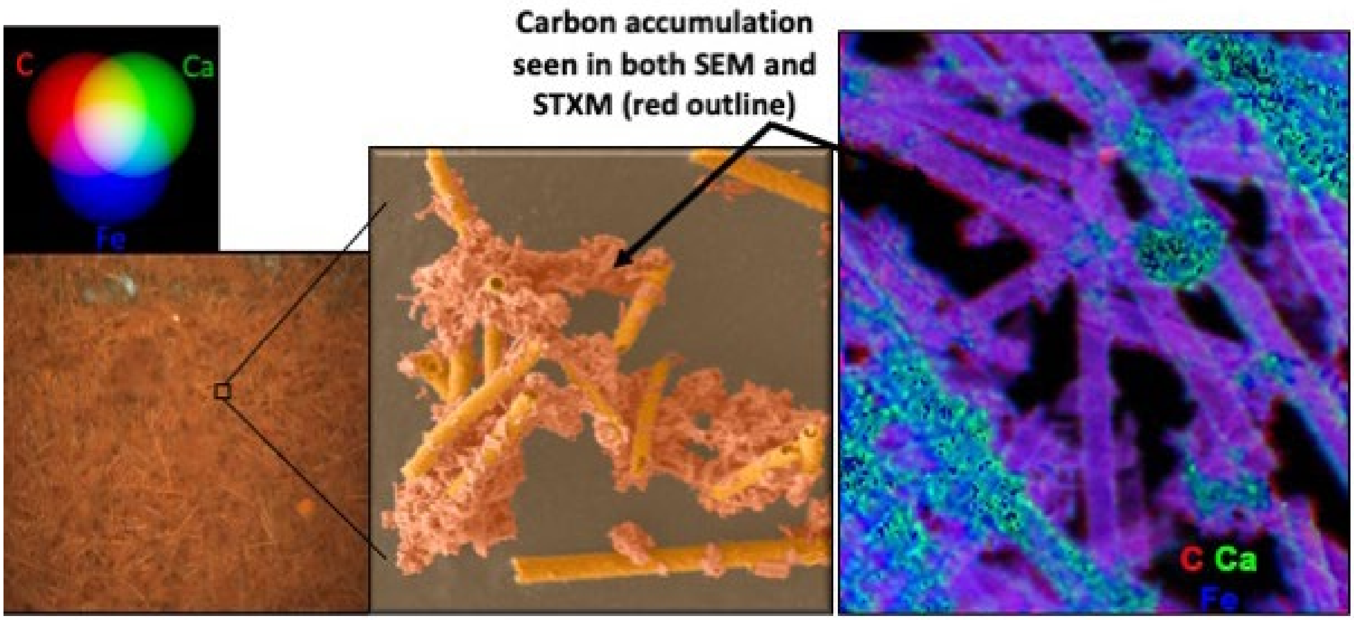

https://doi.org/10.1021/acs.est.9b00540

ADVANCED MATERIALS

Efficient electrocatalytic conversion of carbon monoxide to propanol using fragmented copper

Yuanjie Pang, Jun Li, Ziyun Wang, Chih-Shan Tan, Pei-Lun Hsieh, Tao-Tao Zhuang, Zhi-Qin Liang, Chengqin Zou, Xue Wang, Phil De Luna, Jonathan P. Edwards, Yi Xu, Fengwang Li, Cao-Thang Dinh, Miao Zhong, Yuanhao Lou, Dan Wu, Lih-Juann Chen, Edward H. Sargent & David Sinton

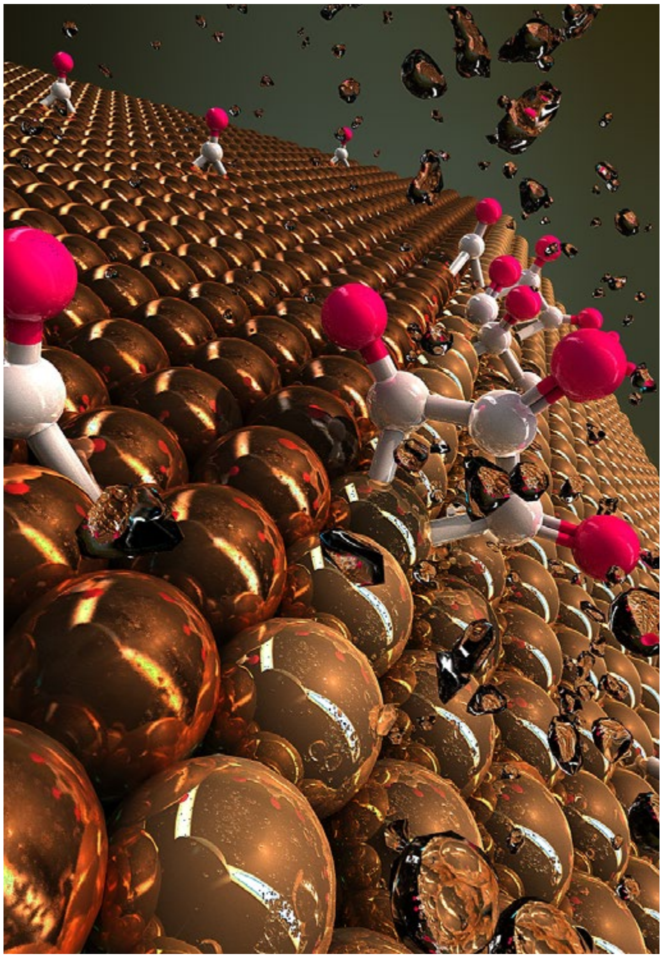

CLS@APS

This work address the active site and formation pathway of copper electrocatalysts to convert carbon dioxide and carbon monoxide into n-propanol, an alcohol that can be directly used as engine fuel.

The renewable-energy-powered electrocatalytic conversion of carbon dioxide and carbon monoxide into carbon-based fuels provides a means for the storage of renewable energy. We sought to convert carbon monoxide—an increasingly available and low-cost feedstock that could benefit from an energy-efficient upgrade in value—into n-propanol, an alcohol that can be directly used as engine fuel. Here we report that a catalyst consisting of highly fragmented copper structures can bring C1 and C2 binding sites together, and thereby promote further coupling of these intermediates into n-propanol. Using this strategy, we achieved an n-propanol selectivity of 20% Faradaic efficiency at a low potential of –0.45 V versus the reversible hydrogen electrode (ohmic corrected) with a full-cell energetic efficiency of 10.8%. We achieved a high reaction rate that corresponds to a partial current density of 8.5 mA cm^{-2} for n-propanol.

https://doi.org/10.1038/s41929-019-0225-7

Photochemically cross-linked quantum well ligands for 2D/3D perovskite photovoltaics with improved photovoltage and stability

Andrew H. Proppe, Mingyang Wei, Bin Chen, Rafael Quintero-Bermudez, Shana O. Kelley, Edward H. Sargent

HXMA

The deployment of perovskite solar cells will rely on further progress in the operating and ambient stability of active layers and interfaces within these materials. Low-dimensional perovskites, also known as perovskite quantum wells (PQWs), utilize organic ligands to protect the perovskite lattice from degradation and offer to improve device stability; combining 2D and 3D perovskites in heterostructures has been shown to take advantage of the high efficiency of the majority 3D active layers and combine it with the improved stability of a thin 2D top layer. Prior PQWs have relied on relatively weak interwell van der Waals bonding between hydrophobic organic moieties of the ligands. Here we instead use the ligand 4-vinylbenzylammonium to form well-ordered PQWs atop a 3D perovskite layer. The ligand's vinyl group is activated using UV light which photochemically forms new covalent bonds among PQWs. UV-cross-linked 2D/3D devices show improved operational stability as well as improved long-term dark stability in air: they retain 90% of their initial efficiency after 2300 h of dark aging compared to a retention of 20% of performance in the case of 3D films. The UV-cross-linked PQWs and 2D/3D interfaces reduce device hysteresis and improve the open-circuit voltages to values up to 1.20 V, resulting in more efficient devices (PCE of up to 20.4%). This work highlights the exploitation of the chemical reactivity of PQW ligands to tailor the molecular properties of PQW interfaces for improved stability and performance in 2D/3D perovskite photovoltaics.

Perovskites are an inexpensive and highly-efficient material for next generation solar cells. This research traces the structural evolution during spin-coating of perovskite film.

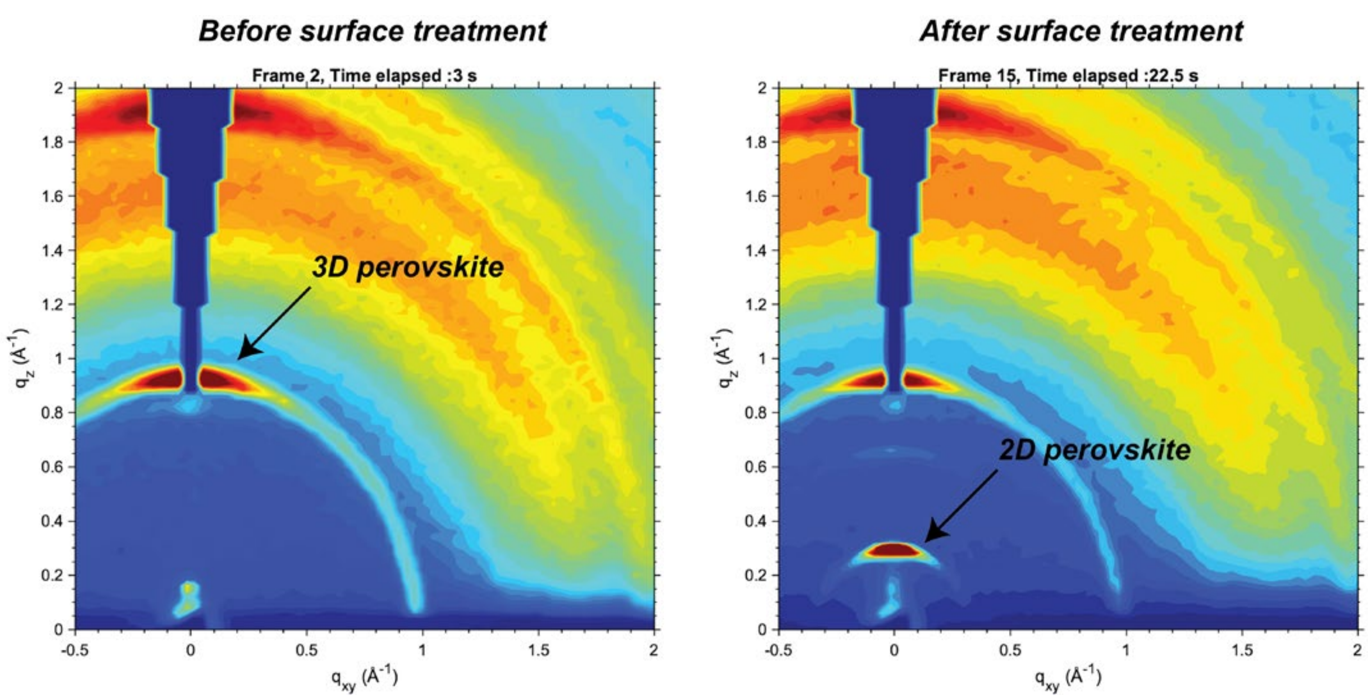

When bulk 3D perovskite surfaces are treated with solutions containing ammonium ligands, a portion of the top surface layer is converted into 2D perovskites, or perovskite quantum wells. These 2D/3D perovskite interfaces have been shown to improve device stability and efficiency. However, the mechanism of 2D/3D interface formation remains unclear. At the HXMA beamline, the CLS helped us to implement in situ spinning GIWAXS experiments, whereby we can collect GIWAXS patterns during the surface treatment process to directly observe the formation of 2D perovskites on the 3D surface, and capture any transient intermediate species. In our recently published paper, we found that our new ligand, 4-vinylbenzylammonium, led to the formation of highly ordered 2D layers after spin coating onto the perovskite surface without any thermal annealing, meaning these low-dimensional structures form immediately during solvent drying. We also observed an intermediate state that was only visible in the first few seconds of spinning. More recent measurements on the Brockhouse beamline gave us access to faster readout times which enabled better time resolution of these intermediate species. Our future studies will focus on trying to resolve the origin and structure of these intermediate species, and employing complementary in situ optical techniques.

https://doi.org/10.1021/jacs.9b05083

Low-profile artificial grid dielectric resonator antenna arrays for mm-wave applications

Highly innovative antenna structures that would be applicable for the coming 5G cell phone networks.

Waqas Mazhar, David M. Klymyshyn, Garth Wells, Aqeel A. Qureshi, Michael Jacobs, Sven Achenbach

SyLMAND

Wideband artificial grid dielectric resonator antenna (GDRA) arrays at 32 GHz for mm-wave applications are presented. The antenna array comprised a GDRA layer and a substrate-integrated waveguide feeding layer. The GDRA array layer is built by embedding small rectangular metal grid structures in low-permittivity dielectric polymethyl methacrylate (PMMA) using deep X-ray lithography (DXRL) and electroforming. The rectangular metallic inclusions significantly increase the effective permittivity of the base material up to 17 by creating high electric flux density regions inside. Low-loss substrate-integrated waveguide (SIW) feeding with longitudinal slots is utilized to excite the GDRA array layer. A 200 μm-thin perforated layer of PMMA is applied between the rectangular grid structures and the SIW feedlines to avoid shorting the metal inclusions to the excitation slots while improving broadband energy coupling to the GDRA layer. The size of the single GDRA array element is only 2.7 mm × 2.7 mm × 0.5 mm (0.29λ o ×0.29λ o ×0.05λ o). Four-element (1×4) and eight-element (1 × 8) GDRA arrays have been fabricated and measured. A measured impedance bandwidth of 6 GHz with a broadside peak gain of 12 dBi and 76% measured radiation efficiency is obtained at 32 GHz for the 1 × 8 GDRA array.

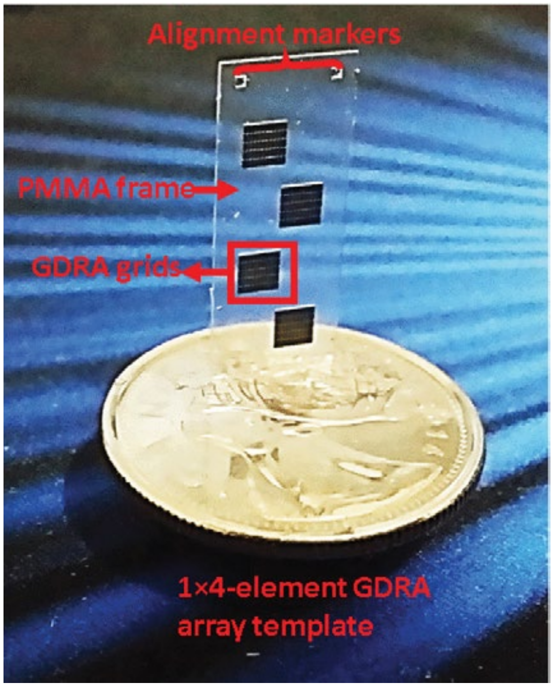

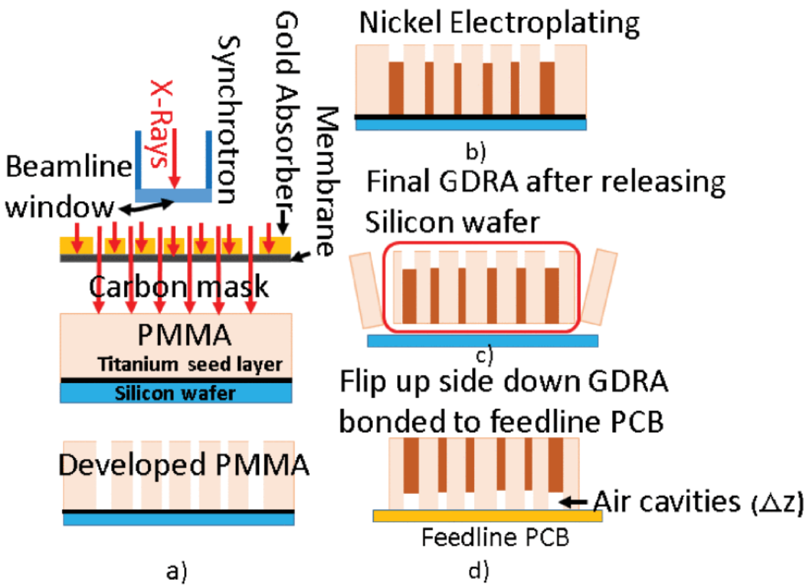

Monolithic four-element embedded GDRA array template.

Embedded GDRA fabrication process. (a) X-ray exposure and development of the PMMA template. (b) Metal electroplating of exposed cavities. (c) Release of the template with embedded GDRA elements from a silicon wafer. (d) Final GDRA mounted on the feedline circuit.

https://doi.org/10.1109/TAP.2019.2907610

Itinerancy-dependent noncollinear spin textures in $SrFeO_3$, $CaFeO_3$, and $CaFeO_3$/$SrFeO_3$ heterostructures probed via resonant x-ray scattering

Paul C. Rogge, Robert J. Green, Ronny Sutarto, and Steven J. May

REIXS

Noncollinear, multi-q spin textures can give rise to exotic, topologically protected spin structures such as skyrmions, but the reason for their formation over simple single-q structures is not well understood. While lattice frustration and the Dzyaloshinskii-Moriya interaction are known to produce noncollinear spin textures, the role of electron itinerancy in multi-q formation is much less studied. Here we investigated the noncollinear, helical spin structures in epitaxial films of the perovskite oxides $SrFeO_3$ and $CaFeO_3$ using magnetotransport and resonant soft x-ray magnetic diffraction. Metallic $SrFeO_3$ exhibits features in its magnetoresistance that are consistent with its recently proposed multi-q structure. Additionally, the magnetic Bragg peak of $SrFeO_3$ measured at the Fe L-edge resonance energy asymmetrically broadens with decreasing temperature in its multi-q state. In contrast, insulating $CaFeO_3$ has a symmetric scattering peak with an intensity 10 times weaker than $SrFeO_3$. Enhanced magnetic scattering at O K-edge prepeak energies demonstrates the role of a negative charge-transfer energy and the resulting oxygen ligand holes in the magnetic ordering of these ferrates. By measuring the magnetic diffraction of $CaFeO_3$/$SrFeO_3$ superlattices with thick $CaFeO_3$ layers, we find that the $CaFeO^3$ helical ordering is coherent across 1-unit-cell-thick $SrFeO_3$ layers but not 6-unit-cell-thick layers. We conclude that insulating $CaFeO_3$ supports only a simple single-q helical structure, in contrast to metallic $SrFeO_3$ that hosts multi-q structures. Our results provide important insight into the role of electron itinerancy in the formation of multi-q spin structures.

There is growing interest in understanding exotic magnetic structures, such as spin spirals and skyrmions, both as a platform to study the fundamental physical interactions that give rise to magnetism in materials and for potential use in information processing and storage. The work suggests new design principles for engineering complex magnetic states, beyond conventional ferro- and antiferromagnets, in metal oxide materials.

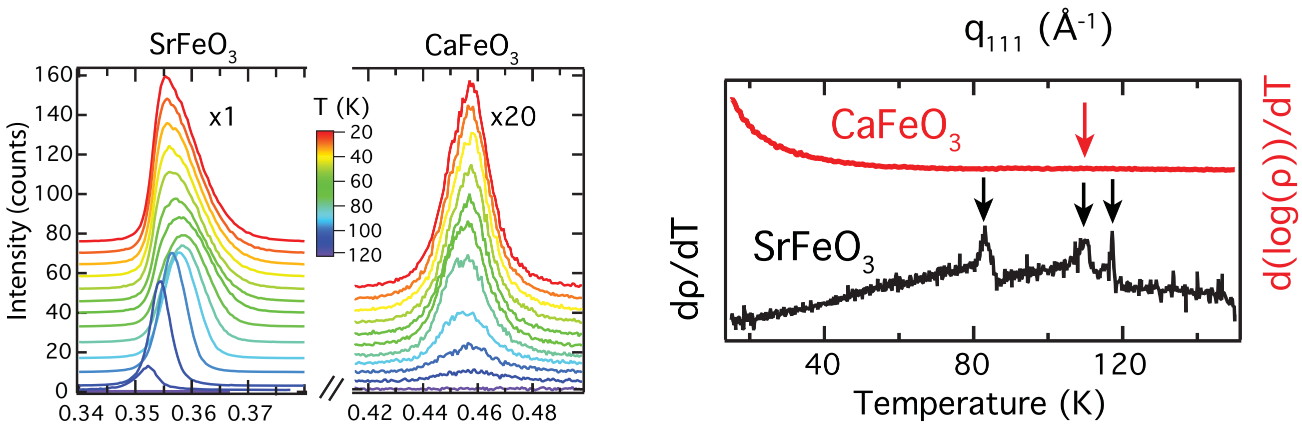

Resonant magnetic scattering along qH=K=L for the $CaFeO_3$ film (E = 710.8 eV) and the $SrFeO_3$ film (E = 710.6 eV), right. Data are offset in y. Using resonant x-ray diffraction, researchers have shown that the helical magnetic state found in iron-based perovskites is dependent on if the material is an insulator such as $CaFeO_3$ or a metal such as $SrFeO_3$. The scattering results suggest that the metallic state stabilizes a highly complex spin structure in $SrFeO_3$ consisting of multiple helices, with evidence for three distinct phases having different helical arrangements.

https://doi.org/10.1103/physrevmaterials.3.084404

PUBLICATIONS

PEER-REVIEWED ARTICLES

Acksel, Andre; Giani, Luise; Stasch, Carolin; Kühn, Peter; Eiter, Sebastian et al. (2019). Humus-rich topsoils in SW Norway – Molecular and isotopic signatures of soil organic matter as indicators for anthropo-pedogenesis. Catena 172, 831-845. DOI: 10.1016/j.catena.2018.09.005.

Acksel, Andre; Baumann, Karen; Hu et al. (2019). A critical review and evaluation of some P-research methods. Communications in Soil Science and Plant Analysis, 1-21. DOI:10.1080/00103624.2019.1679165.

Acksel, Baumann; Hu; Leinweber (2019). A Look into the Past: Tracing Ancient Sustainable Manuring Practices by Thorough P Speciation of Northern European. Soil Systems 3(4), 72. DOI:10.3390/soilsystems3040072.

Afroz, Sharmin; Brownlie, Robert; Fodje, Michel et al. (2019). The bovine herpesvirus-1 major tegument protein, VP8, interacts with host HSP60 concomitant with deregulation of mitochondrial function. Virus Research 261, 37-49. DOI: 10.1016/j.virusres.2018.12.006.

Aggett, Rebecca; Mallette, Evan; Gilbert, Stephanie E.; Vachon, Melody A.; Schroeter, Kurt L. et al. (2019). The steroid side-chain–cleaving aldolase Ltp2–ChsH2DUF35 is a thiolase superfamily member with a radically repurposed active site. Journal of Biological Chemistry 294(31), jbc.RA119.008889. DOI: 10.1074/jbc.ra119.008889. [PDB: 6ok1]

Aghbolaghy, M.; Ghavami, M.; Soltan, J.; Chen, N. (2019). Effect of active metal loading on catalyst structure and performance in room temperature oxidation of acetone by ozone. Journal of Industrial and Engineering Chemistry 77, 118-127. DOI: 10.1016/j.jiec.2019.04.026.

Aimon, Akfiny Hasdi; Hidayat; Rahmat; Rahmawati et al. (2019). Facile deposition of reduced graphene oxide-based transparent conductive film with microwave assisted method. Thin Solid Films 692, 137618. DOI: 10.1016/j.tsf.2019.137618.

Alleon, Julien; Flannery, David T.; Ferralis et al. (2019). Organo-mineral associations in chert of the 3.5 Ga Mount Ada Basalt raise questions about the origin of organic matter in Paleoarchean hydrothermally influenced sediments. Scientific Reports 9(1). DOI: 10.1038/s41598-019-53272-5.

Almawi, Ahmad W; Scotland, Michelle K; Randall, Justin R; Liu, Linda; Martin, Heather K et al. (2019). Binding of the regulatory domain of MutL to the sliding β-clamp is species specific. Nucleic Acids Research 47(9). DOI: 10.1093/nar/gkz115.

Alwani, Saniya; Hua, QingYun; Iftikhar et al. (2019). Lysine functionalized nanodiamonds as gene carriers - Investigation of internalization pathways and intracellular trafficking. Diamond and Related Materials 98, 107477. DOI: 10.1016/j.diamond.2019.107477.

Amin, M. Ruhul; de Boer, T.; Becker, Peter; Hertrampf, Jan; Niewa, Rainer et al. (2019). Bandgap and Electronic Structure Determination of Oxygen-Containing Ammonothermal InN: Experiment and Theory. Journal of Physical Chemistry C 123(14), 8943-8950. DOI: 10.1021/acs.jpcc.8b12369.

Andersen, Amity; Rajput, Nav Nidhi; Han, Kee Sung; Pan, Huilin; Govind, Niranjan et al. (2019). Structure and Dynamics of Polysulfide Clusters in a Nonaqueous Solvent Mixture of 1,3-Dioxolane and 1,2-Dimethoxyethane. Chemistry of Materials 31(7), 2308-2319. DOI: 10.1021/acs.chemmater.8b03944.

Arnal, Gregory; Stogios, Peter J.; Asohan, Jathavan; Attia, Mohamed; Skarina, Tatiana et al. (2019). Substrate specificity, regiospecificity, and processivity in glycoside hydrolase family 74. Journal of Biological Chemistry, jbc.RA119.009861. DOI: 10.1074/jbc.ra119.009861.

Atake, Oghenevwogaga J.; Cooper, David M.L.; Eames, B. Frank (2019). Bone-like features in skate suggest a novel elasmobranch synapomorphy and deep homology of trabecular mineralization patterns. Acta Biomaterialia 84, 424-436. DOI: 10.1016/j.actbio.2018.11.047.

Azargohar, Ramin; Nanda, Sonil; Kang, Kang; Bond, Toby; Karunakaran, Chithra et al. (2019). Effects of bio-additives on the physicochemical properties and mechanical behavior of canola hull fuel pellets. Renewable Energy 132, 296-307. DOI: 10.1016/j.renene.2018.08.003.

Azargohar, Ramin; Soleimani, Majid; Nosran, Shivam; Bond, Toby; Karunakaran, Chithra et al. (2019). Thermo-physical characterization of torrefied fuel pellet from co-pelletization of canola hulls and meal. Industrial Crops and Products 128, 424-435. DOI: 10.1016/j.indcrop.2018.11.042.

Bukejs, Andris; Alekseev, Vitalii I.; Cooper, David M.L.; King, Gavin A.; Mckellar, Ryan C. et al. (2019). A new fossil species of Pycnomerus Erichson (Coleoptera: Zopheridae) from Baltic amber, and a replacement name for a Recent North American congener. Zootaxa 4550(4), 565. DOI : 10.11646/zootaxa.4550.4.6.

Bamford, Natalie C.; Le Mauff, François; Subramanian, Adithya S.; Yip, Patrick; Millán, Claudia et al. (2019). Ega3 from the fungal pathogen Aspergillus fumigatus is an endo-α-1,4-galactosaminidase that disrupts microbial biofilms. Journal of Biological Chemistry 294(37), 13833-13849. DOI: 10.1074/jbc.ra119.009910.

Barbi, Mauricio; Bell, Phil R.; Fanti, Federico; Dynes, James J.; Kolaceke, Anezka et al. (2019). Integumentary structure and composition in an exceptionally well-preserved hadrosaur (Dinosauria: Ornithischia). PeerJ 7, e7875. DOI: 10.7717/peerj.7875.

Battrell, Logan; Patel, Virat; Zhu, Ning; Zhang, Lifeng; Anderson, Ryan et al. (2019). Imaging of the desaturation of gas diffusion layers by synchrotron computed tomography. Journal of Power Sources 416, 155-162. DOI: 10.1016/j.jpowsour.2019.01.089.

Baumann, Karen; Siebers, Meike; Kruse, Jens; Eckhardt, Kai-Uwe; Hu, Yongfeng et al. (2019). Biological soil crusts as key player in biogeochemical P cycling during pedogenesis of sandy substrate. Geoderma 338, 145-158. DOI: 10.1016/j.geoderma.2018.11.034.

Beam, Jeremiah C.; Hehn, Atikin G.; Grosvenor, Andrew P. (2019). Mixed valence cerium substitution in Gd2-xCexTi2O7+δ pyrochlores. Journal of Electron Spectroscopy and Related Phenomena 234. DOI: 10.1016/j.elspec.2019.05.004.

Bellini, Marco; Folliero, Maria G.; Evangelisti, Claudio; He, Qinggang; Hu, Yongfeng et al. (2019). A Gold–Palladium Nanoparticle Alloy Catalyst for CO Production from CO_2 Electroreduction. Energy Technology 7(4), 1800859. DOI: 10.1002/ente.201800859.

Bernath, Peter F.; Bittner, Dror M.; Sibert III, Edwin L. (2019). Isobutane Infrared Bands: Partial Rotational Assignments, ab Initio Calculations, and Local Mode Analysis. Journal of Physical Chemistry A 123(29), 6185-6193. DOI: 10.1021/acs.jpca.9b03321.

Bevilacqua, Nico; Eifert, László; Banerjee, Rupak; Köble, Kerstin; Faragó, Tomáš et al. (2019). Visualization of electrolyte flow in vanadium redox flow batteries using synchrotron X-ray radiography and tomography – Impact of electrolyte species and electrode compression. Journal of Power Sources 439, 227071. DOI: 10.1016/j.jpowsour.2019.227071.

Bian, Juanjuan; Cheng, Xiaopeng; Meng, Xiaoyi; Wang, Jian; Zhou, Jigang et al. (2019). Nitrogen-Doped $NiCo_2O_4$ Microsphere as an Efficient Catalyst for Flexible Rechargeable Zinc–Air Batteries and Self-Charging Power System. ACS Applied Energy Materials 2(3), 2296-2304. DOI: 10.1021/acsaem.9b00120.

Bian, Juanjuan; Su, Rui; Yao, Yuan; Wang, Jian; Zhou, Jigang et al. (2019). Mg Doped Perovskite $LaNiO_3$ Nanofibers as an Efficient Bifunctional Catalyst for Rechargeable Zinc–Air Batteries. ACS Applied Energy Materials 2(1), 923-931. DOI: 10.1021/acsaem.8b02183.

Bieringer, Mario; Stewart, J. Ross; Grosvenor, Andrew P.; Dragomir, Mirela; Greedan, John E. et al. (2019). Quenching of Long Range Order and the Mn^{3+} Ordered Moment in the Layered Antiferromagnet, $Ba_xSr_{1-x}LaMnO_4$. A Polarized Neutron Scattering Study. Inorganic Chemistry 58(7), 4300-4309. DOI: 10.1021/acs.inorgchem.8b03419.

Bryan, Marian C.; Drobnick, Joy; Gobbi, Alberto; Kolesnikov, Aleksandr; Chen, Yongsheng et al. (2019). Development of Potent and Selective Pyrazolopyrimidine IRAK4 Inhibitors. Journal of Medicinal Chemistry 62(13). DOI: 10.1021/acs.jmedchem.9b00439.

Canè, E.; Di Lonardo, G.; Fusina, L.; Tamassia, F.; Predoi-Cross, A. et al. (2019). The v2 = 1, 2 and v4 = 1 bending states of $^{15}NH_3$ and their analysis at experimental accuracy. Journal of Chemical Physics 150(19), 194301. DOI: 10.1063/1.5088751.

Cao, Chuntian; Toney, Michael F.; Sham, Tsun-Kong; Harder, Ross; Shearing, Paul R. et al. (2019). Emerging X-ray imaging technologies for energy materials. Materials Today. DOI: 10.1016/j.mattod.2019.08.011.

Carrière, C.; Dillmann, P.; Foy, E.; Neff, D.; Dynes, J.J. et al. (2019). Use of nanoprobes to identify iron-silicates in a glass/iron/argillite system in deep geological disposal. Corrosion Science 158, 108104. DOI: 10.1016/j.corsci.2019.108104.

Caveney, Nathanael A.; Caballero, Guillermo; Voedts, Henri; Niciforovic, Ana; Worrall, Liam J. et al. (2019). Structural insight into YcbB-mediated beta-lactam resistance in Escherichia coli. Nature Communications 10(1). DOI: 10.1038/s41467-019-09507-0.

Caveney, Nathanael A.; Pavlin, Anja; Caballero, Guillermo; Bahun, Miha; Hodnik, Vesna et al. (2019). Structural Insights into Bacteriophage GIL01 gp7 Inhibition of Host LexA Repressor. Structure 27(7). DOI: 10.1016/j.str.2019.03.019.

Chen, Xiujuan; Huang, Gordon; An, Chunjiang; Feng, Renfei; Wu, Yinghui et al. (2019). Plasma-induced PAA-ZnO coated PVDF membrane for oily wastewater treatment: Preparation, optimization, and characterization through Taguchi OA design and synchrotron-based X-ray analysis. Journal of Membrane Science 582, 70-82. DOI: 10.1016/j.memsci.2019.03.091.

Chen, Xiujuan; Huang, Gordon; An, Chunjiang; Feng, Renfei; Yao, Yao et al. (2019). Plasma-induced poly(acrylic acid)-TiO_2 coated polyvinylidene fluoride membrane for produced water treatment: Synchrotron X-Ray, optimization, and insight studies. Journal of Cleaner Production 227, 772-783. DOI: 10.1016/j.jclepro.2019.04.226.

Chen, Yu Seby; Kozlov, Guennadi; Fakih et al. (2019). Mg^{2+}-ATP Sensing in CNNM, a Putative Magnesium Transporter. Structure. DOI: 10.1016/j.str.2019.11.016.

Cosmidis, Julie; Nims, Christine W.; Diercks, David; Templeton, Alexis S. (2019). Formation and stabilization of elemental sulfur through organomineralization. Geochimica et Cosmochimica Acta 247, 59-82. DOI: 10.1016/j.gca.2018.12.025.

Dawczyk, Joanna; Russo, Joe; Spikes, Hugh (2019). Ethoxylated Amine Friction Modifiers and ZDDP. Tribology Letters 67(4). DOI: 10.1007/s11249-019-1221-4.

Deng, Yijie; Chi, Bin; Li, Jing; Wang, Guanghua; Zheng, Long et al. (2019). Atomic Fe-Doped MOF-Derived Carbon Polyhedrons with High Active-

Center Density and Ultra-High Performance toward PEM Fuel Cells. Advanced Energy Materials 9(13), 1802856. DOI: 10.1002/aenm.201802856.

Ding, Jie; Guan, Yong; Cong et al. (2019). Single-Particle Analysis for Structure and Iron Chemistry of Atmospheric Particulate Matter. Analytical Chemistry 92(1), 975-982. DOI: 10.1021/acs.analchem.9b03913.

Dobrică, E.; Le Guillou, C.; Brearley, A.J. (2019). Aqueous alteration of porous microchondrules in Semarkona: Implications for hydration, oxidation and elemental exchange processes. Geochimica et Cosmochimica Acta 244, 292-307. DOI: 10.1016/j.gca.2018.10.002.

Dolgova, Natalia V.; Nehzati, Susan; MacDonald, Tracy C.; Summers, Kelly L.; Crawford, Andrew M. et al. (2019). Disruption of selenium transport and function is a major contributor to mercury toxicity in zebrafish larvae. Metallomics 11(3). DOI: 10.1039/c8mt00315g.

Doyle, Liam; Ovchinnikova, Olga G.; Myler, Katharine; Mallette, Evan; Huang, Bo-Shun et al. (2019). Biosynthesis of a conserved glycolipid anchor for Gram-negative bacterial capsules. Nature Chemical Biology 15(6). DOI: 10.1038/s41589-019-0276-8.

Dragomir, Mirela; Dube, Paul A.; Arčon, Iztok; Boyer, Chad; Rutherford, Megan et al. (2019). Comparing Magnetism in Isostructural Oxides A0.8La1.2MnO4.1: Anisotropic Spin Glass (A = Ba) versus Long-Range Order (A = Sr). Chemistry of Materials 31(19), 7833-7844. DOI: 10.1021/acs.chemmater.9b01466.

Du, Yi-Ling; Higgins, Melanie A.; Zhao, Guiyun; Ryan, Katherine S. (2019). Convergent biosynthetic transformations to a bacterial specialized metabolite. Nature Chemical Biology. DOI: 10.1038/s41589-019-0331-5. [PDB: 6p29]

Dydula, Christopher; Belev, George; Johns, Paul C. (2019). Development and assessment of a multi-beam continuous-phantom-motion x-ray scatter projection imaging system. Review of Scientific Instruments 90(3), 035104-1 - 035104-13. DOI: 10.1063/1.5043393.

Elikem, Essouassi; Laird, Brian D.; Hamilton, Jordan G.; Stewart, Katherine J.; Siciliano, Steven D. et al. (2019). Effects of chemical speciation on the bioaccessibility of zinc in spiked and smelter-affected soils. Environmental Toxicology and Chemistry 38(2). DOI: 10.1002/etc.4328.

Enghag, Sara; Strömbäck, Karin; Li et al. (2019). Incus Necrosis and Blood Supply. Otology and Neurotology 40(7), e713–e722. DOI: 10.1097/mao.0000000000002292.

Etschmann, Barbara; Liu, Weihua; Mayanovic, Robert; Mei, Yuan; Heald, Steven et al. (2019). Zinc transport in hydrothermal fluids: On the roles of pressure and sulfur vs. chlorine complexing. American Mineralogist 104(1), 158-161. 10.2138/am-2019-6719.

Feng, Yuting; Park, Jaeok; Li et al. (2019). Chirality-Driven Mode of Binding of α-Aminophosphonic Acid-Based Allosteric Inhibitors of the Human Farnesyl Pyrophosphate Synthase (hFPPS). Journal of Medicinal Chemistry 62(21), 9691-9702. DOI: 10.1021/acs.jmedchem.9b01104.

Fraund, Matthew; Park, Tim; Yao, Lin; Bonanno, Daniel; Pham, Don Q. et al. (2019). Quantitative capabilities of STXM to measure spatially resolved organic volume fractions of mixedorganicthin sp;⁄thinsp;inorganic particles. Atmospheric Measurement Techniques 12(3), 1619-1633. 10.5194/amt-12-1619-2019.

Fu, Yanqing; Wei, Qiliang; Zhang, Gaixia; Zhong, Yu; Moghimian, Nima et al. (2019). LiFePO4-Graphene Composites as High-Performance Cathodes for Lithium-Ion Batteries: The Impact of Size and Morphology of Graphene. Materials 12(6), 842. 10.3390/ma12060842.

Gagarina, Varvara; Bojagora, Anna; Lacdao et al. (2019). Structural Basis of the Interaction Between Ubiquitin Specific Protease 7 and Enhancer of Zeste Homolog 2. Journal of Molecular Biology. DOI: 10.1016/j.jmb.2019.12.026.

Gagnon, Vincent; Button, Mark; Boparai et al. (2019). Influence of realistic wearing on the morphology and release of silver nanomaterials from textiles. Environmental Science: Nano 6(2), 411-424. DOI: 10.1039/c8en00803e.

Gao, Jinglin; Boahene, Philip Effah; Hu et al. (2019). Atomic Layer Deposition ZnO Over-Coated Cu/SiO_2 Catalysts for Methanol Synthesis from CO_2 Hydrogenation. Catalysts 9(11), 922. 10.3390/catal9110922.

Garcia Arredondo, Mariela; Lawrence, Corey R.; Schulz, Marjorie S.; Tfaily, Malak M.; Kukkadapu, Ravi et al. (2019). Root-driven weathering impacts on mineral-organic associations in deep soils over pedogenic time scales. Geochimica et Cosmochimica Acta 263, 68-84. DOI: 10.1016/j.gca.2019.07.030.

Garside, E.L.; Whelan, T.A.; Stark, M.R.; Rader, S.D.; Fast, N.M. et al. (2019). Prp8 in a Reduced Spliceosome Lacks a Conserved Toggle that Correlates with Splicing Complexity across Diverse Taxa. Journal of Molecular Biology 431(14). DOI: 10.1016/j.jmb.2019.04.047.

Gassaway, Brandon M.; Cardone, Rebecca L.; Padyana et al. (2019). Distinct Hepatic PKA and CDK Signaling Pathways Control Activity-Independent Pyruvate Kinase Phosphorylation and Hepatic Glucose Production. Cell Reports 29(11), 3394-3404.e9. DOI: 10.1016/j.celrep.2019.11.009.

Ge, N.; Banerjee, R.; Muirhead, D.; Lee, J.; Liu, H. et al. (2019). Membrane dehydration with increasing current density at high inlet gas relative humidity in polymer electrolyte membrane fuel cells. Journal of Power Sources 422, 163-174. DOI: 10.1016/j.jpowsour.2019.03.001.

Ge, N.; Chevalier, S.; Muirhead et al. (2019). Detecting cathode corrosion in polymer electrolyte membrane fuel cells in dead-ended anode mode via alternating current impedance. Journal of Power Sources 439, 227089. DOI: 10.1016/j.jpowsour.2019.227089.

Ge, N.; Shrestha, P.; Balakrishnan et al. (2019). Resolving the gas diffusion layer substrate land and channel region contributions to the oxygen transport resistance of a partially-saturated substrate. Electrochimica Acta 328, 135001. DOI: 10.1016/j.electacta.2019.135001.

Geiger; Michael; Brown; Chris; Wichers et al. (2019). Structural insights into PfARO and characterization of its interaction with PfAIP. Journal of Molecular Biology. DOI: 10.1016/j.jmb.2019.12.024.

Gherase; Mihai R.; Fleming; David E. B. (2019). Probing Trace Elements in Human Tissues with Synchrotron Radiation. Crystals 10(1), 12. 10.3390/cryst10010012.

Ghiasi, Mahnaz; Hariki, Atsushi; Winder, Mathias; Kuneš, Jan; Regoutz, Anna et al. (2019). Charge-transfer effect in hard x-ray 1s and 2p photoemission spectra: LDA+DMFT and cluster-model analysis. Physical Review B 100(7). 10.1103/physrevb.100.075146.

Glæsner, Nadia; Hansen, Hans Christian Bruun; Hu, Yongfeng; Bekiaris, Georgios; Bruun, Sander et al. (2019). Low crystalline apatite in bone char produced at low temperature ameliorates phosphorus-deficient soils. Chemosphere 223, 723-730. DOI: 10.1016/j.chemosphere.2019.02.048.

Gourgas, Ophélie; Muiznieks, Lisa D.; Bello et al. (2019). Cross-Linked Elastin-like Polypeptide Membranes as a Model for Medial Arterial Calcification. Biomacromolecules 20(7), 2625-2636. DOI: 10.1021/acs.biomac.9b00417.

Gu, Chunhao; Hart, Stephen C.; Turner, Benjamin L.; Hu, Yongfeng; Meng, Yong et al. (2019). Aeolian dust deposition and the perturbation of phosphorus transformations during long-term ecosystem development in a cool, semi-arid environment. Geochimica et Cosmochimica Acta 246, 498-514. DOI: 10.1016/j.gca.2018.12.017.

Guo, Xiaoxuan; Situm, Arthur; Barlow, Burke C.; Guo, Bao; Burgess, Ian J. et al. (2019). Soft X-ray spectromicroscopy studies of pitting corrosion of reinforcing steel bar. Surface and Interface Analysis 51(6), 681-691. DOI: 10.1002/sia.6640.

Gytz, Heidi; Liang, Jason; Liang, Yingke; Gorelik, Alexei; Illes, Katalin et al. (2019). The structure of mammalian β-mannosidase provides insight into β-mannosidosis and nystagmus. FEBS Journal 286(7). 10.1111/febs.14731.

Haji-Ghassemi, Omid; Yuchi, Zhiguang; Van Petegem, Filip (2019). The Cardiac Ryanodine Receptor Phosphorylation Hotspot Embraces PKA in a Phosphorylation-Dependent Manner. Molecular Cell 75(1). DOI: 10.1016/j.molcel.2019.04.019.

Hamilton, Jordan G.; Grosskleg, Jay; Hilger, David; Dhillon, Gurbir Singh; Bradshaw, Kris et al. (2019). In situ transformations of bonechar and tri-poly phosphate amendments in phosphorus-limited subsurface soils. Applied Geochemistry 109, 104398. DOI: 10.1016/j.apgeochem.2019.104398.

He, Peng; Jarvis, Jack S.; Meng, Shijun; Li, Qingyin; Bernard, Guy M. et al. (2019). Co-aromatization of methane with propane over Zn/HZSM-5: The methane reaction pathway and the effect of Zn distribution. Applied Catalysis B: Environmental 250, 99-111. DOI: 10.1016/j.apcatb.2019.03.011.

He, Peng; Jarvis, Jack; Liu, Lijia; Song, Hua (2019). The promoting effect of Pt on the co-aromatization of pentane with methane and propane over Zn-Pt/HZSM-5. Fuel 239, 946-954. DOI: 10.1016/j.fuel.2018.11.079.

He, Peng; Wang, Aiguo; Meng, Shijun; Bernard, Guy M.; Liu, Lijia et al. (2019). Impact of Al sites on the methane co-aromatization with alkanes over Zn/HZSM-5. Catalysis Today 323. DOI: 10.1016/j.cattod.2018.05.051.

Henderson, Eric J.; Helwig, Kate; Read, Stuart; Rosendahl, Scott M. (2019). Infrared chemical mapping of degradation products in cross-sections from paintings and painted objects. Heritage Science 7(1). DOI: 10.1186/s40494-019-0313-7.

Herrmann, Jonathan; Li, Po-Nan; Jabbarpour et al. (2019). A bacterial surface layer protein exploits multistep crystallization for rapid self-assembly. Proceedings of the National Academy of Sciences of the United States of America 117(1), 388-394. DOI: 10.1073/pnas.1909798116.

Hestrin, Rachel; Torres-Rojas, Dorisel; Dynes, James J.; Hook, James M.; Regier, Tom Z. et al. (2019). Fire-derived organic matter retains ammonia through covalent bond formation. Nature Communications 10(1). DOI: 10.1038/s41467-019-08401-z.

Hettle; Andrew G.; Hobbs; Joanne K.; Pluvinage et al. (2019). Insights into the κ/ι-carrageenan metabolism pathway of some marine Pseudoalteromonas species. Communications Biology 2(474). DOI: 10.1038/s42003-019-0721-y.

Hewett, D.M.; Bernath, P.F.; Billinghurst, B.B. (2019). Infrared absorption cross sections of isobutane with hydrogen and nitrogen as broadening gases. Journal of Quantitative Spectroscopy and Radiative Transfer 227, 226-229. DOI: 10.1016/j.jqsrt.2019.02.008.

Hewett; Dan; Bernath; Peter F.; Wong et al. (2019). N_2 and H_2 broadened isobutane infrared absorption cross sections and butane upper limits on Titan. Icarus, 113460. DOI: 10.1016/j.icarus.2019.113460.

Hitchcock, Adam P.; Wang, Xiaoyue; Grandfield, Kathryn; Everett, James; Collingwood, Joanna F. et al. (2019). Correlative Spectromicroscopy and Tomography for Biomedical Applications Involving

Electron, Ion, and Soft X-ray Microscopies. Microscopy Today 27(2), 12-19. DOI: 10.1017/s1551929518001256.

Ho, J.; Becker, J.; Leedahl, B.; Boukhvalov, D. W.; Zhidkov, I. S. et al. (2019). Electronic structure and structural defects in 3d-metal doped In_2O_3. Journal of Materials Science Materials in Electronics 30(15), 14091-14098. DOI: 10.1007/s10854-019-01775-2.

Hobbs, Joanne K.; Pluvinage, Benjamin; Robb, Melissa; Smith, Steven P.; Boraston, Alisdair B. et al. (2019). Two complementary α-fucosidases from Streptococcus pneumoniae promote complete degradation of host-derived carbohydrate antigens. Journal of Biological Chemistry 294(34), jbc. RA119.009368. DOI: 10.1074/jbc.ra119.009368. [PDB: 6or4]

Huang, Ji; Nguyen, Vinh H.; Hamblin, Karleigh A.; Maytum, Robin; van der Giezen, Mark et al. (2019). ATP-specificity of succinyl-CoA synthetase from Blastocystis hominis. Acta Crystallographica Section D: Structural Biology 75(7), 647-659. DOI: 10.1107/s2059798319007976.

Huang; Jing; Huang, Guohe; An, Chunjiang et al. (2019). Exploring the use of ceramic disk filter coated with Ag/ZnO nanocomposites as an innovative approach for removing Escherichia coli from household drinking water. Chemosphere, 125545. DOI: 10.1016/j.chemosphere.2019.125545.

Hull, Killian; Wells, Tyler; Billinghurst, Brant E.; Bunn, Hayley; Raston, Paul L. et al. (2019). Synchrotron-based infrared spectroscopy of formic acid: Confirmation of the reassignment of Fermi-coupled 8 μm states. AIP Advances 9(1), 015021. DOI: 10.1063/1.5063010.

Ilyas; Azhar; Velton; Megen; Shah et al. (2019). Rapid Regeneration of Vascularized Bone by Nanofabricated Amorphous Silicon Oxynitrophosphide (SiONP) Overlays. Journal of Biomedical Nanotechnology 15(6), 1241-1255. DOI: 10.1166/jbn.2019.2779.

Ishizawa, Jo; Zarabi, Sarah F.; Davis, R. Eric; Halgas, Ondrej; Nii, Takenobu et al. (2019). Mitochondrial ClpP-Mediated Proteolysis Induces Selective Cancer Cell Lethality. Cancer Cell 35(5). DOI: 10.1016/j.ccell.2019.03.014.

Izadifar; Zahra; Babyn; Paul; Chapman et al. (2019). Ultrasound Cavitation/Microbubble Detection and Medical Applications. Journal of Medical and Biological Engineering 39(3), 259–276. DOI: 10.1007/s40846-018-0391-0.

Izawa, Matthew R. M.; Dynes, James J.; Banerjee, Neil R.; Flemming, Roberta L.; MacLean, Lachlan C. W. et al. (2019). Organic Matter Preservation and Incipient Mineralization of Microtubules in 120 Ma Basaltic Glass. Frontiers in Earth Science 7. DOI: 10.3389/feart.2019.00149.

Jamwal, Ankur; Saibu, Yusuf; MacDonald, Tracy C.; George, Graham N.; Niyogi, Som et al. (2019). The effects of dietary selenomethionine on tissue-specific accumulation and toxicity of dietary arsenite in rainbow trout (Oncorhynchus mykiss) during chronic exposure. Metallomics 11(3), 643-655. DOI: 10.1039/c8mt00309b.

Jiang, Yi; Deng, Ya-Ping; Liang, Ruilin; Fu, Jing; Luo, Dan et al. (2019). Multidimensional Ordered Bifunctional Air Electrode Enables Flash Reactants Shuttling for High-Energy Flexible Zn-Air Batteries. Advanced Energy Materials 9(24), 1900911. DOI: 10.1002/aenm.201900911.

Jiang, Kun; Back, Seoin; Akey, Austin J. et al. (2019). Highly selective oxygen reduction to hydrogen peroxide on transition metal single atom coordination. Nature Communications 10(1). DOI: 10.1038/s41467-019-11992-2.

Jiang, Peng; Zhao, Jinxian; Han et al. (2019). Highly Active and Dispersed Ni/Al2O3 Catalysts for CO Methanation Prepared by the Cation–Anion Double-Hydrolysis Method: Effects of Zr, Fe, and Ce Promoters. Industrial & Engineering Chemistry Research 58(27), 11728-11738. DOI: 10.1021/acs.iecr.9b00002.

Jiang; Qingzheng; He; Lunke; Rehman et al. (2019). Optimized composition and improved magnetic properties of Ce-Fe-B alloys. Journal of Alloys and Compounds 811, 151998. DOI: 10.1016/j.jallcom.2019.151998.

Jones; Darryl R.; McLean, Richard; Hobbs, Joanne K. et al. (2019). A surrogate structural platform informed by ancestral reconstruction and resurrection of a putative carbohydrate binding module hybrid illuminates the neofunctionalization of a pectate lyase. Journal of Structural Biology 207(3), 279-286. DOI: 10.1016/j.jsb.2019.06.003.

Juvvadi, Praveen R.; Fox, David; Bobay, Benjamin G.; Hoy, Michael J.; Gobeil, Sophie M. C. et al. (2019). Harnessing calcineurin-FK506-FKBP12 crystal structures from invasive fungal pathogens to develop antifungal agents. Nature Communications 10(1). DOI: 10.1038/s41467-019-12199-1.

Kang, Mingu; Pelliciari, Jonathan; Frano, Alex; Breznay, Nicholas; Schierle, Enrico et al. (2019). Evolution of charge order topology across a magnetic phase transition in cuprate superconductors. Nature Physics 15(4), 335-340. DOI: 10.1038/s41567-018-0401-8.

Kaplan, Daniel I.; Price, Kimberly A.; Xu, Chen; Li, Dien; Lin, Peng et al. (2019). Iodine speciation in a silver-amended cementitious system. Environment International 126, 576-584. DOI: 10.1016/j.envint.2019.02.070.

Karunakaran, Chithra; Vijayan, Perumal; Stobbs, Jarvis et al. (2019). High throughput nutritional profiling of pea seeds using Fourier transform mid-infrared spectroscopy. Food Chemistry 125585. DOI: 10.1016/j.foodchem.2019.125585.

Keegan, Brenna C.; Ocampo, Daniel; Shearer, Jason (2019). pH Dependent Reversible Formation of a Binuclear Ni_2 Metal-Center within a Peptide Scaffold. Inorganics 7(7), 90. DOI: 10.3390/inorganics7070090.

Khorshid, Mohammad Said Hamma; Kruse, Jens; Semella, Sebastian; Vohland, Michael; Wagner, Jean-Frank et al. (2019). Phosphorus fractions and speciation in rural and urban calcareous soils in the semiarid region of Sulaimani city, Kurdistan, Iraq. Environmental Earth Sciences 78(16). DOI: 10.1007/s12665-019-8543-2.

Kim, Chang-Yong; Cui, Xiaoyu; Cho, Jinchul; Choi, Jeong-Yong; Kim, Hyun-Tak et al. (2019). X-ray induced vanadium $L_3M_{23}M_{45}$ auger electron spectra as tool to trace vanadium oxidation state: Study of surface stoichiometry recovery of V_2O_3 film. Surfaces and Interfaces 15, 26-29. DOI: 10.1016/j.surfin.2019.02.003.

King, Graham; Garcia-Martin, Susana (2019). Expanding the Doubly Cation Ordered AA'BB'O_6 Perovskite Family: Structural Complexity in $NaLaInNbO_6$ and $NaLaInTaO_6$. Inorganic Chemistry 58(20), 14058-14067. DOI: 10.1021/acs.inorgchem.9b02050.

Kirkey, Aaron; Li, Jun; Sham, T.K. (2019). Low temperature amorphous to anatase phase transition of titanium oxide nanotubes. Surface Science 680, 68-74. DOI: 10.1016/j.susc.2018.10.012.

Kleebusch, Enrico; Patzig, Christian; Krause et al. (2019). The titanium coordination state and its temporal evolution in Li_2O–Al_2O_3–SiO_2 (LAS) glasses with ZrO_2 and TiO_2 as nucleation agents - A XANES investigation. Ceramics International. DOI: 10.1016/j.ceramint.2019.10.064.

Kotiuga, Michele; Zhang, Zhen; Li et al. (2019). Carrier localization in perovskite nickelates from oxygen vacancies. Proceedings of the National Academy of Sciences of the United States of America, 201910490. DOI: 10.1073/pnas.1910490116.

Kozachuk, M. S.; Sham, T. K.; Martin, R. R.; Nelson, A. J.; Coulthard, I. et al. (2019). Eyeing the past: synchrotron μ-XANES and XRF imaging of tarnish distribution on 19th century daguerreotypes. Journal of Synchrotron Radiation 26(5), 1679-1686. DO: 10.1107/s1600577519006313.

Kozachuk, Madalena S.; Sham, Tsun-Kong; Martin, Ronald R.; Nelson, Andrew J.; Coulthard, Ian et al. (2019). Recovering Past Reflections: X-Ray Fluorescence Imaging of Electrocleaned 19th Century Daguerreotypes. Heritage 2(1), 568-586. DOI:10.3390/heritage2010037.

Kruse, Jens; Koch, Maximilian; Minh Khoi et al. (2019). Land use change from permanent rice to alternating rice-shrimp or permanent shrimp in the coastal Mekong Delta, Vietnam: Changes in the nutrient status and binding forms. Science of the Total Environment, 134758. DOI: 10.1016/j.scitotenv.2019.134758.

Krüger, Peter; Maekawa, Yuya; Hitchcock, Adam; Bittencourt, Carla (2019). Polarization dependent X-ray absorption near-edge spectra of boron nitride nanotubes. Radiation Physics and Chemistry. DOI: 10.1016/j.radphyschem.2019.01.014.

Kuatsjah, Eugene; Verstraete, Meghan M.; Kobylarz, Marek J.; Liu, Alvin K. N.; Murphy, Michael E. P. et al. (2019). Identification of functionally important residues and structural features in a bacterial lignostilbene dioxygenase. Journal of Biological Chemistry 294(35), jbc. RA119.009428. DOI: 10.1074/jbc.ra119.009428.

LaCroix, Rachelle E.; Tfaily, Malak M.; McCreight, Menli; Jones, Morris E.; Spokas, Lesley et al. (2019). Shifting mineral and redox controls on carbon cycling in seasonally flooded mineral soils. Biogeosciences 16(13), 2573-2589. DOI: 10.5194/bg-16-2573-2019.

Labiuk, Shaunivan L.; Sygusch, Jurgen; Grochulski, Pawel (2019). Structures of soluble rabbit neprilysin complexed with phosphoramidon or thiorphan. Acta Crystallographica Section F: Structural Biology Communications 75(6), 405-411. DOI: 10.1107/s2053230x19006046.

Lang, Dean E.; Morris, Jeremy S.; Rowley, Michael; Torres, Miguel A.; Maksimovich, Vook A. et al. (2019). Structure–function studies of tetrahydroprotoberberine N-methyltransferase reveal the molecular basis of stereoselective substrate recognition. Journal of Biological Chemistry 294(40), jbc. RA119.009214. DOI: 10.1074/jbc.ra119.009214.

Le Nagard, Lucas; Yu, Liu; Rajkotwala, Murtuza; Barkley, Solomon; Bazylinski, Dennis A et al. (2019). Misalignment between the magnetic dipole moment and the cell axis in the magnetotactic bacterium Magnetospirillum magneticum AMB-1. Physical Biology 16(6). DOI: 10.1088/1478-3975/ab2858.

Lee, J.; Liu, H.; George, M.G.; Banerjee, R.; Ge, N. et al. (2019). Microporous layer to carbon fibre substrate interface impact on polymer electrolyte membrane fuel cell performance. Journal of Power Sources 422, 113-121. DOI: 10.1016/j.jpowsour.2019.02.099.

Leedahl, B.; McCloskey, D. J.; Boukhvalov, D. W.; Zhidkov, I. S.; Kukharenko, A. I. et al. (2019). Fundamental crystal field excitations in magnetic semiconductor SnO_2: Mn, Fe, Co, Ni. Physical Chemistry Chemical Physics 21(22), 11992-11998. DOI: 10.1039/c9cp01516g.

Leedahl, Brett; de Boer, Tristan; Yuan, Xiaotao; Moewes, Alexander (2019). Oxygen Vacancy Induced Structural Distortions in Black Titania: A Unique Approach using Soft X-ray EXAFS at the O-K Edge. Chemistry - A European Journal 25(13), 3272-3278. DOI: 10.1002/chem.201805423.

Lees, R.M.; Reid, E.M; Xu et al. (2019). Synchrotron spectroscopy of the CSH-bending and CH_3-rocking bands of methyl mercaptan. Canadian Journal of Physics, 1-11. 10.1139/cjp-2019-0487.

Lei, Ming; Tempel, Wolfram; Chen et al. (2019). Plasticity at the DNA recognition site of the $MeCP_2$ mCG-binding domain. Biochimica et

Biophysica Acta (BBA) - Gene Regulatory Mechanisms 1862(9), 194409. DOI: 10.1016/j.bbagrm.2019.194409.

Lepot, Kevin; Williford, Kenneth H.; Philippot, Pascal; Thomazo, Christophe; Ushikubo, Takayuki et al. (2019). Extreme 13C-depletions and organic sulfur content argue for S-fueled anaerobic methane oxidation in 2.72 Ga old stromatolites. Geochimica et Cosmochimica Acta 244, 522-547. DOI: 10.1016/j.gca.2018.10.014.

Li, Dien; Seaman, John C.; Hunyadi Murph, Simona E.; Kaplan, Daniel I.; Taylor-Pashow, Kathryn et al. (2019). Porous iron material for TcO_4^- and ReO_4^- sequestration from groundwater under ambient oxic conditions. Journal of Hazardous Materials 374, 177-185. DOI: 10.1016/j.jhazmat.2019.04.030.

Li, Dien; Xu, Chen; Yeager, Chris M.; Lin, Peng; Xing, Wei et al. (2019). Molecular Interaction of Aqueous Iodine Species with Humic Acid Studied by I and C K-Edge X-ray Absorption Spectroscopy. Environmental Science & Technology. DOI: 10.1021/acs.est.9b03682.

Li, Jia; Jia, Yunhua; Lin, Aiyang; Hanna, Michelle; Chelico, Linda et al. (2019). Structure of Ddi2, a highly inducible detoxifying metalloenzyme from Saccharomyces cerevisiae. Journal of Biological Chemistry 294(27), 10674-10685. DOI: 10.1074/jbc.ra118.006394.

Li, Junrui; Jilani, Safia Z.; Lin, Honghong; Liu, Xiaoming; Wei, Kecheng et al. (2019). Ternary CoPtAu Nanoparticles as a General Catalyst for Highly Efficient Electro-oxidation of Liquid Fuels. Angewandte Chemie 131(33). DOI: 10.1002/ange.201906137.

Li, Junrui; Sharma, Shubham; Liu, Xiaoming; Pan, Yung-Tin; Spendelow, Jacob S. et al. (2019). Hard-Magnet L10-CoPt Nanoparticles Advance Fuel Cell Catalysis. Joule 3(1), 124-135. DOI: 10.1016/j.joule.2018.09.016.

Li, Qi; Liu, Xiangsi; Han, Xiang; Xiang, Yuxuan; Zhong, Guiming et al. (2019). Identification of the Solid Electrolyte Interface on the Si/C Composite Anode with FEC as the Additive. ACS Applied Materials & Interfaces 11(15). DOI: 10.1021/acsami.8b22221.

Li, Tang; Stephen, Preyesh; Zhu, Dao-Wei; Shi, Rong; Lin, Sheng-Xiang et al. (2019). Crystal structures of human 17β-hydroxysteroid dehydrogenase type 1 complexed with estrone and NADP + reveal the mechanism of substrate inhibition. FEBS Journal 286(11). DOI: 10.1111/febs.14784.

Li, Xia; Deng, Sixu; Banis, Mohammad Norouzi; Doyle-Davis, Kieran; Zhang, Dongxing et al. (2019). Suppressing Corrosion of Aluminum Foils via Highly Conductive Graphene-like Carbon Coating in High-Performance Lithium-Based Batteries. ACS Applied Materials & Interfaces 11(36), 32826-32832. DOI: 10.1021/acsami.9b06442.

Li, Xiaona; Liang, Jianwen; Chen, Ning; Luo, Jing; Adair, Keegan R. et al. (2019). Water-Mediated Synthesis of a Superionic Halide Solid Electrolyte. Angewandte Chemie - International Edition. DOI: 10.1002/anie.201909805.

Li, Yan; Liu, Feifei; Xu, Xiaoming; Liu, Yuwei; Li, Yanzhang et al. (2019). Influence of heavy metal sorption pathway on the structure of biogenic birnessite: Insight from the band structure and photostability. Geochimica et Cosmochimica Acta 256. DOI: 10.1016/j.gca.2018.12.008.

Li, Yanzhang; Li, Yan; Xu, Xiaoming; Ding, Cong; Chen, Ning et al. (2019). Structural disorder controlled oxygen vacancy and photocatalytic activity of spinel-type minerals: A case study of $ZnFe_2O_4$. Chemical Geology 504. DOI: 10.1016/j.chemgeo.2018.11.022.

Li, Yuguang C.; Wang, Ziyun; Yuan, Tiange; Nam, Dae-Hyun; Luo, Mingchuan et al. (2019). Binding Site Diversity Promotes CO_2 Electroreduction to Ethanol. Journal of the American Chemical Society 141(21), 8584-8591. DOI: 10.1021/jacs.9b02945.

Li, Chen; Zhu, Ning; Emady et al. (2019). Synchrotron-based X-ray in-situ imaging techniques for advancing the understanding of pharmaceutical granulation. International Journal of Pharmaceutics 572, 118797. DOI: 10.1016/j.ijpharm.2019.118797.

Li, Fengmiao; Davidson, Bruce A.; Sutarto et al. (2019). Epitaxial growth of perovskite $SrBiO_3$ film on $SrTiO_3$ by oxide molecular beam epitaxy. Physical Review Materials 3(10). 10.1103/physrevmaterials.3.100802.

Li, Liang; Castro, Fernando C.; Park et al. (2019). Probing Electrochemically Induced Structural Evolution and Oxygen Redox Reactions in Layered Lithium Iridate. Chemistry of Materials 31(12), 4341-4352. DOI: 10.1021/acs.chemmater.8b04591.

Li, Zhejun; Jiang, Haoran; Lai et al. (2019). Designing Effective Solvent–Catalyst Interface for Catalytic Sulfur Conversion in Lithium–Sulfur Batteries. Chemistry of Materials 31(24), 10186-10196. DOI: 10.1021/acs.chemmater.9b03885.

Li, Zhijie; Tomlinson, Aidan CA; Wong et al. (2019). The human coronavirus HCoV-229E S-protein structure and receptor binding. eLife 8. DOI: 10.7554/elife.51230.

Liang, Jianwen; Li, Xiaona; Zhao, Yang; Goncharova, Lyudmila V.; Li, Weihan et al. (2019). An Air-Stable and Dendrite-Free Li Anode for Highly Stable All-Solid-State Sulfide-Based Li Batteries. Advanced Energy Materials 9(38), 1902125. DOI: 10.1002/aenm.201902125.

Lin, Jinru; Nilges, Mark J.; Wiens, Eli; Chen, Ning; Wang, Shaofeng et al. (2019). Mechanism of Gd3+ uptake in gypsum (CaSO4·2H2O): Implications for EPR dating, REE recovery and REE behavior. Geochimica et Cosmochimica Acta 258, 63-78. DOI: 10.1016/j.gca.2019.05.019.

Lin, Xiao; Zhou, Jing; Zheng, Dehua; Guan, Chengzhi; Xiao, Guoping et al. (2019). Rational synthesis of CaCo2O4 nanoplate as an earth-abundant electrocatalyst for oxygen evolution reaction. Journal of Energy Chemistry 31, 125-131. DOI: 10.1016/j.jechem.2018.05.015.

Liu, Peng; Ptacek, Carol J.; Blowes, David W.; Finfrock, Y. Zou (2019). Mercury distribution and speciation in biochar particles reacted with contaminated sediment up to 1030 days: A synchrotron-based study. Science of the Total Environment 662, 915-922. DOI: 10.1016/j.scitotenv.2019.01.148.

Liu, Peng; Ptacek, Carol J.; Blowes, David W.; Finfrock, Y. Zou; Steinepreis, Mark et al. (2019). A Method for Redox Mapping by Confocal Micro-X-ray Fluorescence Imaging: Using Chromium Species in a Biochar Particle as an Example. Analytical Chemistry 91(8), 5142-5149. DOI: 10.1021/acs.analchem.8b05718.

Liu, Yanli; Qin, Su; Chen, Tsai-Yu; Lei, Ming; Dhar, Shilpa S. et al. (2019). Structural insights into trans-histone regulation of H3K4 methylation by unique histone H4 binding of MLL3/4. Nature Communications 10(1). DOI: 10.1038/s41467-018-07906-3. [PDB: 6mlc]

Liu, Jin; Sui, Peng; Cade-Menun et al. (2019). Molecular-level understanding of phosphorus transformation with long-term phosphorus addition and depletion in an alkaline soil. Geoderma 353, 116-124. DOI: 10.1016/j.geoderma.2019.06.024.

Liu, Lichen; Meira, Debora M.; Arenal et al. (2019). Determination of the Evolution of Heterogeneous Single Metal Atoms and Nanoclusters under Reaction Conditions: Which Are the Working Catalytic Sites?. ACS Catalysis, 10626-10639. DOI: 10.1021/acscatal.9b04214.

Liu, Min; Liu, Mengxia; Wang et al. (2019). Quantum-Dot-Derived Catalysts for CO2 Reduction Reaction. Joule 3(7), 1703-1718. DOI: 10.1016/j.joule.2019.05.010.

Liu, Na; Zhao, Lifang; Tang et al. (2019). Mid-infrared spectroscopy is a fast screening method for selecting Arabidopsis genotypes with altered leaf cuticular wax. Plant. Cell and Environment. DOI: 10.1111/pce.13691.

Liu, Yulong; Banis, Mohammad Norouzi; Xiao et al. (2019). Visualization of the secondary phase in LiFePO4 ingots with advanced mapping techniques. Canadian Journal of Chemical Engineering 97(8), 2218-2223. DOI: 10.1002/cjce.23413.

Liu; Yunqiu; Huang; Gordon; An et al. (2019). Use of Nano-TiO_2 self-assembled flax fiber as a new initiative for immiscible oil/water separation. Journal of Cleaner Production, 119352. DOI: 10.1016/j.jclepro.2019.119352.

Lounsbury, Amanda W.; Wang, Ranran; Plata, Desiree L.; Billmyer, Nicholas; Muhich, Christopher et al. (2019). Preferential adsorption of selenium oxyanions onto {1 1 0} and {0 1 2} nano-hematite facets. Journal of Colloid and Interface Science 537, 465-474. DOI: 10.1016/j.jcis.2018.11.018.

Lu, Anhuai; Li, Yan; Ding, Hongrui; Xu, Xiaoming; Li, Yanzhang et al. (2019). Photoelectric conversion on Earth's surface via widespread Fe- and Mn-mineral coatings. Proceedings of the National Academy of Sciences of the United States of America, 201902473. DOI: 10.1073/pnas.1902473116.

Lu, Bing-Qiang; Garcia, Natalya A.; Chevrier, Daniel M.; Zhang, Peng; Raiteri, Paolo et al. (2019). Short-Range Structure of Amorphous Calcium Hydrogen Phosphate. Crystal Growth & Design 19(5), 3030-3038. DOI: 10.1021/acs.cgd.9b00274.

Lu, Bingzhang; Guo, Lin; Wu, Feng; Peng, Yi; Lu, Jia En et al. (2019). Ruthenium atomically dispersed in carbon outperforms platinum toward hydrogen evolution in alkaline media. Nature Communications 10(1). DOI: 10.1038/s41467-019-08419-3.

Lu, Zhonghui; Duan, James J.-W.; Xiao, Haiyun; Neels, James; Wu, Dauh-Rurng et al. (2019). Identification of potent, selective and orally bioavailable phenyl ((R)-3-phenylpyrrolidin-3-yl) sulfone analogues as RORγt inverse agonists. Bioorganic and Medicinal Chemistry Letters 29(16). DOI: 10.1016/j.bmcl.2019.06.036. [PDB: 6p9f]

Lu, Ziyang; Wang, Bo; Hu, Yongfeng; Liu, Wei; Zhao, Yufeng et al. (2019). An Isolated Zinc–Cobalt Atomic Pair for Highly Active and Durable Oxygen Reduction. Angewandte Chemie 131(9). DOI: 10.1002/ange.201810175.

Luan, Xiaojie; Tam, Julian S.; Belev, George et al. (2019). Nebulized hypertonic saline triggers nervous system-mediated active liquid secretion in cystic fibrosis swine trachea. Scientific Reports 9(1), 540. DOI: 10.1038/s41598-018-36695-4.

Lutfalla, Suzanne; Barré, Pierre; Bernard, Sylvain; Le Guillou, Corentin; Alléon, Julien et al. (2019). Multidecadal persistence of organic matter in soils: multiscale investigations down to the submicron scale. Biogeosciences 16(7), 1401-1410. 10.5194/bg-16-1401-2019.

Ma, Jinjin; Yao, Qianting; McLeod, John A.; Chang, Lo-Yueh; Pao, Chih-Wen et al. (2019). Investigating the luminescence mechanism of Mn-doped $CsPb(Br/Cl)_3$ nanocrystals. Nanoscale 11(13), 6182-6191. DOI: 10.1039/c9nr00143c.

Ma, Limei; Zhang, Xiangzhi; Xu, Zijian; Späth, Andreas; Xing, Zhenjiang et al. (2019). Three-dimensional focal stack imaging in scanning transmission X-ray microscopy with an improved reconstruction algorithm. Optics Express 27(5), 7787. DOI : 10.1364/oe.27.007787.

Mabanglo, Mark F.; Leung, Elisa; Vahidi et al. (2019). ClpP protease activation results from the reorganization of the electrostatic interaction networks at the entrance pores. Communications Biology 2(410). DOI: 10.1038/s42003-019-0656-3.

Mangat, Chand S.; Vadlamani, Grishma; Holicek, Viktor; Chu, Mitchell; Larmour, Veronica L. C. et al. (2019). Molecular Basis for the Potent Inhibition of the Emerging Carbapenemase VCC-1 by Avibactam. Antimicrobial Agents and Chemotherapy 63(4). 10.1128/aac.02112-18.

Marhaba, Iman; Ferry, Daniel; Laffon, Carine; Regier, Thomas Z.; Ouf, François-Xavier et al. (2019). Aircraft and MiniCAST soot at the nanoscale. Combustion and Flame 204, 278-289. DOI: 10.1016/j.combustflame.2019.03.018.

Martens, Isaac; Melo, Lis G. A.; Wilkinson, David P.; Bizzotto, Dan; Hitchcock, Adam P. et al. (2019). Characterization of X-ray Damage to Perfluorosulfonic Acid Using Correlative Microscopy. Journal of Physical Chemistry C 123(26). DOI: 10.1021/acs.jpcc.9b03924.

Martinelli, Michela; Mehrbod, Mohammad; Graham, Uschi M.; Hu, Yongfeng; Gnanamani, Muthu K. et al. (2019). Soft X-ray Characterization of Sulfur-Poisoned Cation-Exchanged Pt/KL Catalysts for Aromatization of Hexane. ACS Symposium Series, 243-260. DOI: 10.1021/bk-2019-1320.ch009.

Mascle; Xavier H.; Gagnon; Christina; Wahba et al. (2019). Acetylation of SUMO1 Alters Interactions with the SIMs of PML and Daxx in a Protein-Specific Manner. Structure. DOI: 10.1016/j.str.2019.11.019.

Mazhar, Waqas; Klymyshyn, David M.; Wells, Garth; Qureshi, Aqeel A.; Jacobs, Michael et al. (2019). Low-Profile Artificial Grid Dielectric Resonator Antenna Arrays for mm-Wave Applications. IEEE Transactions on Antennas and Propagation 67(7), 1-1. 10.1109/tap.2019.2907610.

Mazhar, Waqas; Klymyshyn, David; Wells, Garth; Qureshi, Aqeel; Jacobs, Michael et al. (2019). 60 GHz Substrate Integrated Waveguide-Fed Monolithic Grid Dielectric Resonator Antenna Arrays. IEEE Antennas and Wireless Propagation Letters 18(6), 1109-1113. DOI: 10.1109/lawp.2019.2910255.

McCallum, Matthew; Benlekbir, Samir; Nguyen et al. (2019). Multiple conformations facilitate PilT function in the type IV pilus. Nature Communications 10(5198). DOI: 10.1038/s41467-019-13070-z.

McCaugherty, Sarah; Grosvenor, Andrew P. (2019). Low-temperature synthesis of $CaZrTi_2O_7$ zirconolite-type materials using ceramic, coprecipitation, and sol-gel methods. Journal of Materials Chemistry C 7(1), 177-187. DOI: 10.1039/c8tc04560g.

McLeod, Brandon; Miura, Kazutoyo; Scally, Stephen W.; Bosch, Alexandre; Nguyen, Ngan et al. (2019). Potent antibody lineage against malaria transmission elicited by human vaccination with Pfs25. Nature Communications 10(1). DOI: 10.1038/s41467-019-11980-6.

Mcleod, Matthew J.; Krismanich, Anthony P.; Assoud et al. (2019). Characterization of 3-[(Carboxymethyl)thio] picolinic Acid: A Novel Inhibitor of Phosphoenolpyruvate Carboxykinase. Biochemistry 58(37), 3918-3926. DOI: 10.1021/acs.biochem.9b00583.

Melo, Lis G.A.; Hitchcock, Adam P. (2019). Electron beam damage of perfluorosulfonic acid studied by soft X-ray spectromicroscopy. Micron 121, 8-20. DOI: 10.1016/j.micron.2019.02.006.

Methot, Joey L.; Zhou, Hua; Kattar, Sam D.; McGowan, Meredeth A.; Wilson, Kevin et al. (2019). Structure Overhaul Affords a Potent Purine PI3Kδ Inhibitor with Improved Tolerability. Journal of Medicinal Chemistry 62(9). DOI: 10.1021/acs.jmedchem.8b01818.

Morhart, Tyler A.; Read, Stuart T.; Wells et al. (2019). Micromachined multigroove silicon ATR FT-IR internal reflection elements for chemical imaging of microfluidic devices. Analytical Methods. DOI: 10.1039/c9ay02248a.

Mostafijur Rahman, K.M.; Mohtadi-Bonab, M.A.; Ouellet, Ryan; Szpunar, Jerzy; Zhu, Ning et al. (2019). Effect of electrochemical hydrogen charging on an API X70 pipeline steel with focus on characterization of inclusions. International Journal of Pressure Vessels and Piping 173, 147-155. DOI: 10.1016/j.ijpvp.2019.05.006.

Mothersole, Robert G.; Macdonald, Marta; Kolesnikov, Maxim; Murphy, Michael E. P.; Wolthers, Kirsten R. et al. (2019). Structural insight into the high reduction potentials observed for Fusobacterium nucleatum flavodoxin. Protein Science 28(8). DOI: 10.1002/pro.3661.

Murugesan, Vijayakumar; Gray, Michel; Guo, Mond; Job, Heather; Kovarik, Libor et al. (2019). Thermally activated nucleation and growth of cobalt and nickel oxide nanoparticles on porous silica. Journal of Vacuum Science and Technology A: Vacuum. Surfaces and Films 37(3), 031101. DOI: 10.1116/1.5080448.

Negassa, Wakene; Acksel, Andre; Eckhardt, Kai-Uwe; Regier, Tom; Leinweber, Peter et al. (2019). Soil organic matter characteristics in drained and rewetted peatlands of northern Germany: Chemical and spectroscopic analyses. Geoderma 353, 468-481. DOI: 10.1016/j.geoderma.2019.07.002.

Newson, Joshua P. M.; Scott, Nichollas E.; Yeuk Wah Chung, Ivy; Wong Fok Lung, Tania; Giogha, Cristina et al. (2019). Salmonella Effectors SseK1 and SseK3 Target Death Domain Proteins in the TNF and TRAIL Signaling Pathways*. Molecular Cellular Proteomics 18(6), 1138-1156. DOI: 10.1074/mcp.ra118.001093. [PDB: 6cgi, 6dus]

Nguyen; Vinh H.; Singh; Noreen; Medina et al. (2019). Identification of the active site residues in ATP-citrate lyase's carboxy-terminal portion. Protein Science 28(10), 1840-1849. DOI: 10.1002/pro.3708.

Ning; Liqun; Zhu; Ning; Mohabatpour et al. (2019). Bioprinting Schwann cell-laden scaffolds from low-viscosity hydrogel compositions. Journal of Materials Chemistry B 7(29), 4538-4551. DOI: 10.1039/c9tb00669a.

Norouzi Banis, Mohammad; Wang, Zhiqiang; Rousselot, Steeve; Liu, Yulong; Hu, Yongfeng et al. (2019). Chemical speciation and mapping of the Si in Si doped LFP ingot with synchrotron radiation technique. Canadian Journal of Chemical Engineering 97(8), 2211-2217. DOI: 10.1002/cjce.23430.

Pan, B.Y.; Jang, H.; Lee, J.-S.; Sutarto, R.; He, F. et al. (2019). Intertwined Spin and Orbital Density Waves in MnP Uncovered by Resonant Soft X-Ray Scattering. Physical Review X 9(2). DOI: 10.1103/physrevx.9.021055.

Panahifar; Arash; Chapman; L. Dean; Weber et al. (2019). Biodistribution of strontium and barium in the developing and mature skeleton of rats. Journal of Bone and Mineral Metabolism 37(3), 385–398. DOI: 10.1007/s00774-018-0936-x.

Pang, Yuanjie; Li, Jun; Wang, Ziyun; Tan, Chih-Shan; Hsieh, Pei-Lun et al. (2019). Efficient electrocatalytic conversion of carbon monoxide to propanol using fragmented copper. Nature Catalysis 2(3), 251-258. DOI: 10.1038/s41929-019-0225-7.

Patel, Virat; Battrell, Logan; Anderson et al. (2019). Investigating effect of different gas diffusion layers on water droplet characteristics for proton exchange membrane (PEM) fuel cells. International Journal of Hydrogen Energy 44(33), 18340-18350. DOI: 10.1016/j.ijhydene.2019.05.111.

Pattammattel, Ajith; Leppert, Valerie J.; Forman, Henry Jay; O'Day, Peggy A. (2019). Surface characterization and chemical speciation of adsorbed iron(iii) on oxidized carbon nanoparticles. Environmental Sciences: Processes and Impacts 21(3), 548-563. DOI: 10.1039/c8em00545a.

Perera, Sahan D.; Wang, Jian; Urquhart, Stephen G. (2019). Linear dichroism in the NEXAFS spectra of n-alkane crystalline polymorphs. Journal of Electron Spectroscopy and Related Phenomena 232, 5-10. DOI: 10.1016/j.elspec.2018.12.004.

Perez-Borrajero, Cecilia; Lin, Chang Sheng-Huei; Okon, Mark; Scheu, Karlton; Graves, Barbara J. et al. (2019). The Biophysical Basis for Phosphorylation-Enhanced DNA-Binding Autoinhibition of the ETS1 Transcription Factor. Journal of Molecular Biology 431(3). DOI: 10.1016/j.jmb.2018.12.011.

Peterson, Ronald C.; Metcalf, Mallory; Kampf et al. (2019). Cadwaladerite, $Al_2(H_2O)(OH)_4\cdot n(Cl,OH-,H_2O)$, from Cerros Pintados, Chile, defined as a valid mineral species and the discreditation of lesukite. Canadian Mineralogist 57(6), 827-841. DOI: 10.3749/canmin.1900040.

Picard, Aude; Gartman, Amy; Cosmidis et al. (2019). Authigenic metastable iron sulfide minerals preserve microbial organic carbon in anoxic environments. Chemical Geology 530, 119343. DOI: 10.1016/j.chemgeo.2019.119343.

Pravica, Michael G.; Schyck, Sarah; Harris, Blake; Cifligu, Petrika; Kim, Eunja et al. (2019). Fluorine chemistry at extreme conditions: possible synthesis of HgF_4. Papers in Physics 11, 110001. DOI: 10.4279/pip.110001.

Qamar, Amir; Amin, Muhammad Ruhul; Grynko et al. (2019). A Probe of Valence and Conduction Band Electronic Structure of Lead Oxide Films for Photodetectors. ChemPhysChem 20(24), 3328-3335. DOI: 10.1002/cphc.201900726.

Qi, Peng; Samadi, Nazanin; Martinson, Mercedes et al. (2019). Wide field imaging energy dispersive X-ray absorption spectroscopy. Scientific Reports 9(1), 17734 (1-14). DOI: 10.1038/s41598-019-54287-8.

Rohani, S. Alireza; Iyaniwura, John E.; Zhu et al. (2019). Effects of object-to-detector distance and beam energy on synchrotron radiation phase-contrast imaging of implanted cochleae. Journal of Microscopy 273(2), 127-134. DOI: 10.1111/jmi.12768.

Radka, Christopher D.; Labiuk, Shaunivan L.; DeLucas, Lawrence J.; Aller, Stephen G. (2019). Structures of the substrate-binding protein YfeA in apo and zinc-reconstituted holo forms. Acta Crystallographica Section D: Structural Biology 75(9). DOI: 10.1107/s2059798319010866.

Rahfeld, Peter; Sim, Lyann; Moon, Haisle; Constantinescu, Iren; Morgan-Lang, Connor et al. (2019). An enzymatic pathway in the human gut microbiome that converts A to universal O type blood. Nature Microbiology 4(9). DOI: 10.1038/s41564-019-0469-7.

Rahman, KM Mostafijur; Szpunar, Jerzy; Toroghinejad et al. (2019). Characterization of aluminum/alumina/TiC hybrid composites in 3D produced by anodizing and accumulating roll bonding process using synchrotron radiation tomography. Journal of Composite Materials 53(9), 1215-1227. DOI: 10.1177/0021998318796177.

Raman, Swetha; Beilschmidt, Melissa; To, Minh; Lin, Kevin; Lui, Francine et al. (2019). Structure-guided design fine-tunes pharmacokinetics, tolerability, and antitumor profile of multispecific frizzled antibodies. Proceedings of the National Academy of Sciences of the United States of America 116(14), 6812-6817. DOI: 10.1073/pnas.1817246116. [PDB: 6o39, 6o3a]

Rana, Rachita; Nanda, Sonil; Maclennan, Aimee; Hu, Yongfeng; Kozinski, Janusz A. et al. (2019). Comparative evaluation for catalytic gasification of petroleum coke and asphaltene in subcritical and supercritical water. Journal of Energy Chemistry 31, 107-118. DOI: 10.1016/j.jechem.2018.05.012.

Reid, Joel W.; Kaduk, James A.; Matei, Lidia (2019). The crystal structure of $MoO_2(O_2)(H_2O)\cdot H_2O$. Powder Diffraction 34(1), 44-49. DOI: 10.1017/s0885715619000095.

Reimer; Janice M.; Eivaskhani; Maximilian; Harb et al. (2019). Structures of a dimodular nonribosomal peptide synthetase reveal conformational flexibility. Science 366(6466), eaaw4388. DOI : 10.1126/science.aaw4388.

Rescourio, Gwenaella; Gonzalez, Ana Z.; Jabri et al. (2019). Discovery and in Vivo Evaluation of Macrocyclic

Mcl-1 Inhibitors Featuring an α-Hydroxy Phenylacetic Acid Pharmacophore or Bioisostere. Journal of Medicinal Chemistry 62(22), 10258-10271. DOI: 10.1021/acs.jmedchem.9b01310.

Rice, Kyle; Batul, Kissa; Whiteside et al. (2019). The predominance of nucleotidyl activation in bacterial phosphonate biosynthesis. Nature Communications 10(3698). DOI: 10.1038/s41467-019-11627-6.

Riggs, Jennifer R.; Elsner, Jan; Cashion, Dan; Robinson, Dale; Tehrani, Lida et al. (2019). Design and Optimization Leading to an Orally Active TTK Protein Kinase Inhibitor with Robust Single Agent Efficacy. Journal of Medicinal Chemistry 62(9), 4401-4410. DOI: 10.1021/acs.jmedchem.8b01869.

Robertson, Jared M.; Nesbitt, Jake A.; Lindsay, Matthew B.J. (2019). Aqueous- and solid-phase molybdenum geochemistry of oil sands fluid petroleum coke deposits, Alberta, Canada. Chemosphere 217, 715-723. DOI: 10.1016/j.chemosphere.2018.11.064.

Rogge, Paul C.; Green, Robert J.; Sutarto, Ronny; May, Steven J. (2019). Itinerancy-dependent noncollinear spin textures in $SrFeO_3$, $CaFeO_3$, and $CaFeO_3$/$SrFeO_3$ heterostructures probed via resonant x-ray scattering. Physical Review Materials 3(8). DOI: 10.1103/physrevmaterials.3.084404.

Ross, Michael B.; Li, Yifan; De Luna, Phil; Kim, Dohyung; Sargent, Edward H. et al. (2019). Electrocatalytic Rate Alignment Enhances Syngas Generation. Joule 3(1), 257-264. DOI: 10.1016/j.joule.2018.09.013.

Rozon, Kelsey L.; Banerjee, Neil R.; Van Loon, Lisa L.; Pearson, Bill (2019). Application of Innovative Geochemical and Mineralogical Techniques to Understanding the La Victoria Epithermal Gold Deposit, Peru. Microscopy and Microanalysis 25(S2), 800-801. DOI: 10.1017/s1431927619004732.

Sahtout, Naheda; Kuttiyatveetil, Jijin R.A.; Sanders, David A.R. (2019). Structure and function of the putative thioredoxin 1 from the thermophilic eubacterium Thermosipho africanus strain TCF52B. Biochimica et Biophysica Acta - Proteins and Proteomics 1867(4), 426-433. DOI: 10.1016/j.bbapap.2019.01.011.

Samadi, Nazanin; Shi, Xianbo; Dallin et al. (2019). A real-time phase-space beam emittance monitoring system. Journal of Synchrotron Radiation 26(4), 1213-1219. DOI: 10.1107/s1600577519005423.

Santos, Antonio C. F.; Vasconcelos, Debora N.; MacDonald, Michael A.; Sant'Anna, Marcelo M.; Tenório, Bruno N. C. et al. (2019). Experimental and theoretical results of resonant and normal Auger decay in dichloromethane. European Physical Journal D 73(4). DOI: 10.1140/epjd/e2019-90625-y.

Schaller, Jörg; Faucherre, Samuel; Joss, Hanna; Obst, Martin; Goeckede, Mathias et al. (2019). Silicon increases the phosphorus availability of Arctic soils. Scientific Reports 9(1). DOI: 10.1038/s41598-018-37104-6.

Schart-Morén; Nadine; Agrawal; Sumit K.; Ladak et al. (2019). Effects of Various Trajectories on Tissue Preservation in Cochlear Implant Surgery. Ear and Hearing 40(2), 393–400. DOI: 10.1097/aud.0000000000000624.

Schrag, Joseph D.; Picard, Marie-Ève; Gaudreault, Francis; Gagnon, Louis-Patrick; Baardsnes, Jason et al. (2019). Binding symmetry and surface flexibility mediate antibody self-association. mAbs 11(7), 1-19. DOI:10.1080/19420862.2019.1632114.

Sengupta, Shomit; Giaime, Emilie; Narayan, Sridhar; Hahm, Seung; Howell, Jessica et al. (2019). Discovery of NV-5138, the first selective Brain mTORC1 activator. Scientific Reports 9(1), 4107. DOI: 10.1038/s41598-019-40693-5.

Shadike, Zulipiya; Lee, Hung-Sui; Tian, Chuanjin; Sun, Ke; Song, Liang et al. (2019). Synthesis and Characterization of a Molecularly Designed High-Performance Organodisulfide as Cathode Material for Lithium Batteries. Advanced Energy Materials 9(21), 1900705. DOI: 10.1002/aenm.201900705.

Sharma, Vibhu; Dörr, Nicole; Erdemir, Ali; Aswath, Pranesh B. (2019). Antiwear Properties of Binary Ashless Blend of Phosphonium Ionic Liquids and Borate Esters in Partially Formulated Oil (No Zn). Tribology Letters 67(2). DOI: 10.1007/s11249-019-1152-0.

Sharma, Vinay; Timmons, Richard B.; Erdemir, Ali; Aswath, Pranesh B. (2019). Interaction of plasma functionalized TiO_2 nanoparticles and ZDDP on friction and wear under boundary lubrication. Applied Surface Science 489. DOI: 10.1016/j.apsusc.2019.05.359.

Shen, Yanfeng; Wang, Meijun; Hu, Yongfeng; Kong, Jiao; Wang, Jiancheng et al. (2019). Transformation and regulation of sulfur during pyrolysis of coal blend with high organic-sulfur fat coal. Fuel 249, 427-433. DOI: 10.1016/j.fuel.2019.03.066.

Shi, Rui; Ning, Lixin; Wang, Zhiqiang; Chen, Jiatang; Sham, Tsun-Kong et al. (2019). Zero-Thermal Quenching of Mn^{2+} Red Luminescence via Efficient Energy Transfer from Eu^{2+} in $BaMgP_2$. Advanced Optical Materials, 1901187. DOI: 10.1002/adom.201901187.

Shiri, Sheida; Odeshi, Akindele; Chen, Ning; Feng, Renfei; Sutarto, Ronny et al. (2019). FCC tantalum thin films deposited by magnetron sputtering. Surface and Coatings Technology 358, 942-946. DOI: 10.1016/j.surfcoat.2018.12.015.

Shrestha, Pranay; Ouellette, David; Lee et al. (2019). Graded Microporous Layers for Enhanced Capillary-Driven Liquid Water Removal in Polymer Electrolyte Membrane Fuel Cells. Advanced Materials Interfaces (6), 1901157 (1-10). DOI: 10.1002/admi.201901157.

Siebers, Nina; Kruse, Jens (2019). Short-term impacts of forest clear-cut on soil structure and consequences for organic matter composition and nutrient speciation: A case study. PLoS ONE 14(8), e0220476. DOI: 10.1371/journal.pone.0220476.

Sifat, Rahin; Beam, Jeremiah C.; Grosvenor, Andrew P. (2019). Investigation of Factors That Affect the Oxidation State of Ce in the Garnet-Type Structure. Inorganic Chemistry 58(4). DOI: 10.1021/acs.inorgchem.8b02506.

Simonetta, Kyle R.; Taygerly, Joshua; Boyle, Kathleen; Basham, Stephen E.; Padovani, Chris et al. (2019). Prospective discovery of small molecule enhancers of an E3 ligase-substrate interaction. Nature Communications 10(1), 1402. DOI: 10.1038/s41467-019-09358-9.

Simpson, R.; Varney, T. L.; Swanston et al. (2019). Investigating Past Lead Exposure in Bioarchaeological Remains with Synchrotron X-ray Fluorescence and Absorption Spectroscopy. Synchrotron Radiation News 32(6), 11-16. DOI:10.1080/08940886.2019.1680209.

Situm, Arthur; Guo, Xiaoxuan; Guo, Bao; Barlow, Burke C.; Burgess, Ian J. et al. (2019). A spectromicroscopy study of the corrosion of fusion-bonded epoxy–coated rebar. Surface and Interface Analysis 51(5), 525-530. DOI: 10.1002/sia.6613.

Skierszkan, E.K.; Mayer, K.U.; Weis, D.; Roberston, J.; Beckie, R.D. et al. (2019). Molybdenum stable isotope fractionation during the precipitation of powellite (CaMoO4) and wulfenite (PbMoO4). Geochimica et Cosmochimica Acta 244, 383-402. DOI: 10.1016/j.gca.2018.09.030.

Skierszkan, Elliott K.; Robertson, Jared M.; Lindsay, Matthew B. J.; Stockwell, Justin S.; Dockrey, John W. et al. (2019). Tracing Molybdenum Attenuation in Mining Environments Using Molybdenum Stable Isotopes. Environmental Science & Technology 53(10), 5678-5686. DOI: 10.1021/acs.est.9b00766.

Smith, Bryan D.; Kaufman, Michael D.; Lu, Wei-Ping; Gupta, Anu; Leary, Cynthia B. et al. (2019). Ripretinib (DCC-2618) Is a Switch Control Kinase Inhibitor of a Broad Spectrum of Oncogenic and Drug-Resistant KIT and PDGFRA Variants. Cancer Cell 35(5), 738-751.e9. DOI: 10.1016/j.ccell.2019.04.006.

Smith, Nicholas J.; Regier, Tom; Dutta, Indrajit (2019). Structure and composition of surface depletion layers in poled aluminosilicate glasses. Journal of the American Ceramic Society 102(6), 3037-3062. DOI: 10.1111/jace.16405.

Soltan, Nikoo; Kawalilak, Chantal E.; Cooper, David M.; Kontulainen, Saija A.; Johnston, James D. et al. (2019). Cortical porosity assessment in the distal radius: A comparison of HR-pQCT measures with Synchrotron-Radiation micro-CT-based measures. Bone 120, 439-445. DOI: 10.1016/j.bone.2018.12.008.

Song, Yao; Li, Jing; Peng, Miao; Deng, Ziqi; Yang, Jianjun et al. (2019). Identification of Cr(VI) speciation in ferrous sulfate-reduced chromite ore processing residue (rCOPR) and impacts of environmental factors erosion on Cr(VI) leaching. Journal of Hazardous Materials 373, 389-396. DOI: 10.1016/j.jhazmat.2019.03.097.

Song, Ping; Natale, Giovanniantonio; Wang et al. (2019). 2D and 3D Metal-Organic Framework at the Oil/Water Interface: A Case Study of Copper Benzenedicarboxylate. Advanced Materials Interfaces 6(2), 1801139. DOI: 10.1002/admi.201801139.

Sowers, Tyler D.; Holden, Kathryn L.; Coward, Elizabeth K.; Sparks, Donald L. (2019). Dissolved Organic Matter Sorption and Molecular Fractionation by Naturally Occurring Bacteriogenic Iron (Oxyhydr)oxides. Environmental Science & Technology 53(8), 4295-4304. DOI: 10.1021/acs.est.9b00540.

Spergel, Steven H.; Mertzman, Michael E.; Kempson, James; Guo, Junqing; Stachura, Sylwia et al. (2019). Discovery of a JAK1/3 Inhibitor and Use of a Prodrug to Demonstrate Efficacy in a Model of Rheumatoid Arthritis. ACS Medicinal Chemistry Letters 10(3), 306-311. DOI: 10.1021/acsmedchemlett.8b00508.

Stromberg, Jessica M.; Barr, Erik; Van Loon, Lisa L.; Gordon, Robert A.; Banerjee, Neil R. et al. (2019). Fingerprinting multiple gold mineralization events at the Dome mine in Timmins, Ontario, Canada: Trace element and gold content of pyrite. Ore Geology Reviews 104, 603-619. DOI: 10.1016/j.oregeorev.2018.11.020.

Stromberg, Jessica M.; Van Loon, Lisa L.; Gordon, Robert; Woll, Arthur; Feng, Renfei et al. (2019). Applications of synchrotron X-ray techniques to orogenic gold studies; examples from the Timmins gold camp. Ore Geology Reviews 104, 589-602. DOI: 10.1016/j.oregeorev.2018.11.015.

Strullu-Derrien, Christine; Bernard, Sylvain; Spencer, Alan R. T.; Remusat, Laurent; Kenrick, Paul et al. (2019). On the structure and chemistry of fossils of the earliest woody plant. Palaeontology. DOI: 10.1111/pala.12440.

Sun, Qiming; Wang, Ning; Bai, Risheng; Hui, Yu; Zhang, Tianjun et al. (2019). Synergetic Effect of Ultrasmall Metal Clusters and Zeolites Promoting Hydrogen Generation. Advanced Science 6(10), 1802350. DOI: 10.1002/advs.201802350.

Sun, Wei; D, Lei; Tan et al. (2019). Engineering of Nitrogen Coordinated Single Cobalt Atom Moieties for Oxygen Electroreduction. ACS Applied Materials & Interfaces 11(44), 41258-41266. DOI: 10.1021/acsami.9b11830.

Sun, Xinyang; Scanlon, Martin G.; Guillermic, Reine-Marie et al. (2019). The effects of sodium reduction on the gas phase of bread doughs using synchrotron X-ray microtomography. Food Research International, 108919. DOI: 10.1016/j.foodres.2019.108919.

Tamura, Kazune; Foley, Matthew H.; Gardill, Bernd R.; Dejean, Guillaume; Schnizlein, Matthew et al. (2019). Surface glycan-binding proteins are essential for cereal beta-glucan utilization by the human gut symbiont Bacteroides ovatus. Cellular and Molecular Life Sciences. DOI: 10.1007/s00018-019-03115-3.

Tang; Aimin; Chen; Zhifeng; Cox et al. (2019). A potent broadly neutralizing human RSV antibody targets conserved site IV of the fusion glycoprotein. Nature Communications 10(4153). DOI: 10.1038/s41467-019-12137-1.

Tarry, Michael J.; Harmel, Christoph; Taylor et al. (2019). Structures of GapR reveal a central channel which could accommodate B-DNA. Scientific Reports 9(16679). DOI: 10.1038/s41598-019-52964-2.

Uceda, Marianna; Zhou, Jigang; Wang, Jian; Gauvin, Raynald; Zaghib, Karim et al. (2019). Highly conductive NMP-free carbon-coated nano-lithium titanate/carbon composite electrodes via SBR-assisted electrophoretic deposition. Electrochimica Acta 299, 107-115. DOI: 10.1016/j.electacta.2018.12.166.

Uchagawkar, Anoop; Ramanathan, Anand; Hu, Yongfeng; Subramaniam, Bala (2019). Highly dispersed molybdenum containing mesoporous silicate (Mo-TUD-1) for olefin metathesis. Catalysis Today. DOI: 10.1016/j.cattod.2019.03.073.

Udayakantha, Malsha; Schofield, Parker; Waetzig, Gregory R.; Banerjee, Sarbajit (2019). A full palette: Crystal chemistry, polymorphism, synthetic strategies, and functional applications of lanthanide oxyhalides. Journal of Solid State Chemistry 270, 569-592. DOI: 10.1016/j.jssc.2018.12.017.

Van Loon; Lisa L.; McIntyre; N. Stewart; Bauer et al. (2019). Pekaboo: Advanced software for the interpretation of X-ray fluorescence spectra from synchrotrons and other intense X-ray sources. Software Impacts 2, 100010. DOI: 10.1016/j.simpa.2019.100010.

VanderSchee, Cassidy R.; Kuter, David; Chou, Hsiang; Jackson, Brian P.; Mann, Koren K. et al. (2019). Addressing K/L-edge overlap in elemental analysis from micro-X-ray fluorescence: bioimaging of tungsten and zinc in bone tissue using synchrotron radiation and laser ablation inductively coupled plasma mass spectrometry. Analytical and Bioanalytical Chemistry 412(2), 259-265. DOI: 10.1007/s00216-019-02244-9.

Vanessa; Béland A.; Wang; Zhiqiang; Macdonald et al. (2019). A comprehensive investigation of a zwitterionic Ge(I) dimer with a 1,2-dicationic core. Chemistry - A European Journal. DOI: 10.1002/chem.201903683.

Vasconcelos, D.N.; MacDonald, M.A.; Tenório et al. (2019). Inner-valence Auger decay in chloroform after Cl 2p ionization. Nuclear Instruments and Methods in Physics Research. Section B: Beam Interactions with Materials and Atoms 461, 133-136. DOI: 10.1016/j.nimb.2019.09.039.

Velagapudi, Uday Kiran; Langelier, Marie-France; Delgado-Martin, Cristina; Diolaiti, Morgan E.; Bakker, Sietske et al. (2019). Design and Synthesis of Poly(ADP-ribose) Polymerase Inhibitors: Impact of Adenosine Pocket-Binding Motif Appendage to the 3-Oxo-2,3-dihydrobenzofuran-7-carboxamide on Potency and Selectivity. Journal of Medicinal Chemistry 62(11), 5330-5357. DOI: 10.1021/acs.jmedchem.8b01709.

Vogel, Christian; Sekine, Ryo; Steckenmesser, Daniel; Lombi, Enzo; Herzel, Hannes et al. (2019). Combining diffusive gradients in thin films (DGT) and spectroscopic techniques for the determination of phosphorus species in soils. Analytica Chimica Acta. DOI: 10.1016/j.aca.2019.01.037.

Von Dwingelo, Juanita; Chung, Ivy Yeuk Wah; Price et al. (2019). Interaction of the Ankyrin H Core Effector of Legionella with the Host LARP7 Component of the 7SK snRNP Complex. mBio 10(4), e01942-19. 10.1128/mbio.01942-19.

Vujanovic, Vladimir; Kim, Seon Hwa; Lahlali et al. (2019). Spectroscopy and SEM imaging reveal endosymbiont-dependent components changes in germinating kernel through direct and indirect coleorhiza-fungus interactions under stress. Scientific Reports 9(1). DOI: 10.1038/s41598-018-36621-8.

Vyavhare, Kimaya; Bagi, Sujay; Patel, Mihir; Aswath, Pranesh B. (2019). Impact of Diesel Engine Oil Additives–Soot Interactions on Physiochemical, Oxidation, and Wear Characteristics of Soot. Energy & Fuels 33(5), 4515-4530. DOI: 10.1021/acs.energyfuels.8b03841.

Walsh, Andrew G.; Chen, Ziyi; Zhang et al. (2019). X-ray Spectroscopy of Silver Nanostructures toward Antibacterial Applications. Journal of Physical Chemistry C 124(8), 4339-4351. DOI: 10.1021/acs.jpcc.9b09548.

Wang, Alana O.; Ptacek, Carol J.; Blowes, David W.; Gibson, Blair D.; Landis, Richard C. et al. (2019). Application of hardwood biochar as a reactive capping mat to stabilize mercury derived from contaminated floodplain soil and riverbank sediments. Science of the Total Environment 652, 549-561. DOI: 10.1016/j.scitotenv.2018.10.213.

Wang, Min-Jun; Yu, Fu-Da; Sun, Gang; Wang, Jian; Zhou, Ji-Gang et al. (2019). Co-regulating the surface and bulk structure of Li-rich layered oxides by a phosphor doping strategy for high-energy Li-ion batteries. Journal of Materials Chemistry A 7(14), 8302-8314. DOI: 10.1039/c9ta00783k.

Wang, Sizhe; Liao, Jiaxuan; Yang, Xiaofei; Liang, Jianneng; Sun, Qian et al. (2019). Designing a highly efficient polysulfide conversion catalyst with paramontroseite for high-performance and long-life lithium-sulfur batteries. Nano Energy 57, 230-240. DOI: 10.1016/j.nanoen.2018.12.020.

Wang, Xiang; Jelinski, Nicolas A.; Toner, Brandy; Yoo, Kyungsoo (2019). Long-term agricultural management and erosion change soil organic matter chemistry and association with minerals. Science of the Total Environment 648, 1500-1510. DOI: 10.1016/j.scitotenv.2018.08.110.

Wang, Xiang; Toner, Brandy M.; Yoo, Kyungsoo (2019). Mineral vs. organic matter supply as a limiting factor for the formation of mineral-associated organic matter in forest and agricultural soils. Science of the Total Environment 692, 344-353. DOI: 10.1016/j.scitotenv.2019.07.219.

Wang, Xiaoming; Phillips, Brian; Boily, Jean-François; Hu, Yongfeng; Hu, Zhen et al. (2019). Phosphate Sorption Speciation and Precipitation Mechanisms on Amorphous Aluminum Hydroxide. Soil Systems 3(1), 20. DOI: 10.3390/soilsystems3010020.

Wang, Alana O.; Ptacek, Carol J.; Blowes et al. (2019). Use of hardwood and sulfurized-hardwood biochars as amendments to floodplain soil from South River, VA, USA: Impacts of drying-rewetting on Hg removal. Science of the Total Environment, 136018. DOI: 10.1016/j.scitotenv.2019.136018.

Wei, Qiliang; Cherif, Mohamed; Zhang, Gaixia; Almesrati, Ali; Chen, Jiatang et al. (2019). Transforming reed waste into a highly active metal-free catalyst for oxygen reduction reaction. Nano Energy 62, 700-708. DOI: 10.1016/j.nanoen.2019.05.083.

Wei, Yong; Xiong, Zi Jian; Li, Jun; Zou, Chunxia; Cairo, Christopher W. et al. (2019). Crystal structures of human lysosomal EPDR1 reveal homology with the superfamily of bacterial lipoprotein transporters. Communications Biology 2(1). DOI: 10.1038/s42003-018-0262-9. [PDB: 6e7o]

Wei, Yong; Resetca, Diana; Li et al. (2019). Multiple direct interactions of TBP with the MYC oncoprotein. Nature Structural and Molecular Biology 26(11), 1035-1043. DOI: 10.1038/s41594-019-0321-z.

Wells, Garth; Achenbach, Sven; Subramanian, Venkat; Jacobs, Michael; Klymyshyn, David et al. (2019). SyLMAND: a microfabrication beamline with wide spectral and beam power tuning range at the Canadian Light Source. Journal of Synchrotron Radiation 26(2), 565-570. DOI: 10.1107/s1600577518017721.

Wells, Garth; Achenbach, Sven; Klymyshyn et al. (2019). High-Aspect-Ratio Micropatterning Capabilities into Thick Resist Layers Using Deep X-ray Lithography at SyLMAND. Synchrotron Radiation News 32(4), 44-47. DOI:10.1080/08940886.2019.1634438.

Western, Colin M.; Billinghurst, Brant E. (2019). Automatic and semi-automatic assignment and fitting of spectra with PGOPHER. Physical Chemistry Chemical Physics 21(26). DOI: 10.1039/c8cp06493h.

White, Brandy; Huh, Ian; Brooks et al. (2019). Structure of a VHH isolated from a naïve phage display library. BMC Research Notes 12(154). DOI: 10.1186/s13104-019-4197-0.

Whitesell, Luke; Robbins, Nicole; Huang, David S.; McLellan, Catherine A.; Shekhar-Guturja, Tanvi et al. (2019). Structural basis for species-selective targeting of Hsp90 in a pathogenic fungus. Nature Communications 10(1), 402. DOI: 10.1038/s41467-018-08248-w.

Wong, Andy; Hewett, Dan; Billinghurst, Brant B.; Hodges, James N.; Bernath, Peter F. et al. (2019). He and H^2 broadened propane cross sections in the 3 µm region at cold temperatures. Journal of Quantitative Spectroscopy and Radiative Transfer 232, 104-107. DOI: 10.1016/j.jqsrt.2019.04.038.

Wong, A.K.C.; Ge, N.; Shrestha et al. (2019). Polytetrafluoroethylene content in standalone microporous layers: Tradeoff between membrane hydration and mass transport losses in polymer electrolyte membrane fuel cells. Applied Energy 240, 549-560. DOI: 10.1016/j.apenergy.2019.02.037.

Wrobleski, Stephen T.; Moslin, Ryan; Lin, Shuqun; Zhang, Yanlei; Spergel, Steven et al. (2019). Highly Selective Inhibition of Tyrosine Kinase 2 (TYK2) for the Treatment of Autoimmune Diseases: Discovery of the Allosteric Inhibitor BMS-986165. Journal of Medicinal Chemistry. DOI: 10.1021/acs.jmedchem.9b00444.

Wu, Mingjie; Zhang, Gaixia; Chen, Ning; Chen, Weifeng, Qiao, Jinli et al. (2019). A self-supported electrode as a high-performance binder- and carbon-free cathode for rechargeable hybrid zinc batteries. Energy Storage Materials. DOI: 10.1016/j.ensm.2019.08.009.

Wu, Mingjie; Zhang, Gaixia; Qiao, Jinli; Chen, Ning; Chen, Weifeng et al. (2019). Ultra-long life rechargeable zinc-air battery based on high-performance trimetallic nitride and NCNT hybrid bifunctional electrocatalysts. Nano Energy 61. DOI: 10.1016/j.nanoen.2019.04.031.

Xiao, Wei; Sun, Qian; Banis et al. (2019). Unveiling the Interfacial Instability of the Phosphorus/Carbon Anode for Sodium-Ion Batteries. ACS Applied Materials & Interfaces 11(34), 30763-30773. DOI: 10.1021/acsami.9b07884.

Xin, Xiaying; Huang, Gordon; An, Chunjiang; Feng, Renfei (2019). Interactive Toxicity of Triclosan and Nano-TiO_2 to Green Alga Eremosphaera viridis in Lake Erie: A New Perspective Based on Fourier Transform Infrared Spectromicroscopy and Synchrotron-Based X-ray Fluorescence Imaging. Environmental Science & Technology 53(16), 9884-9894. DOI: 10.1021/acs.est.9b03117.

Xin, Xiaying; Huang, Gordon; An, Chunjiang; Raina-Fulton, Renata; Weger, Harold et al. (2019). Insights into Long-Term Toxicity of Triclosan to Freshwater Green Algae in Lake Erie. Environmental

Science & Technology 53(4), 2189-2198. DOI: 10.1021/acs.est.9b00259.

Xin, Xiaying; Huang, Gordon; An, Chunjiang et al. (2019). Analyzing the Biochemical Alteration of Green Algae During Chronic Exposure to Triclosan Based on Synchrotron-Based Fourier Transform Infrared Spectromicroscopy. Analytical Chemistry 91(12). DOI: 10.1021/acs.analchem.9b01417.

Xu; Shishuai; Gao; Xiang; Deshmukh et al. (2019). Pressure-Promoted Irregular CoMoP2 Nanoparticles Activated by Surface Reconstruction for Oxygen Evolution Reaction Electrocatalyst. Journal of Materials Chemistry A. DOI: 10.1039/c9ta11775j.

Xue, Yuan; Zheng, Li-Li; Wang, Jian; Zhou, Ji-Gang; Yu, Fu-Da et al. (2019). Improving Electrochemical Performance of High-Voltage Spinel LiNi0.5Mn1.5O4 Cathode by Cobalt Surface Modification. ACS Applied Energy Materials 2(4), 2982-2989. DOI: 10.1021/acsaem.9b00564.

Yang, Nuannuan; Guo, Huiqing; Lei, Yanqiu; Zhang, Yanbing; Wang, Meijun et al. (2019). XAS combined with Py-GC study on the effects of temperatures and atmospheres on sulfur release and its transformation behavior during coal pyrolysis. Fuel 250, 373-380. DOI: 10.1016/j.fuel.2019.04.010.

Yin, Penghui; Hegde, Manu; Garnet et al. (2019). Faceting-Controlled Zeeman Splitting in Plasmonic TiO_2 Nanocrystals. Nano Letters 19(9), 6695-6702. DOI: 10.1021/acs.nanolett.9b03128.

Yin, Penghui; Tan, Yi; Ward et al. (2019). Effect of Dopant Activation and Plasmon Damping on Carrier Polarization in In_2O_3 Nanocrystals. Journal of Physical Chemistry C 123(49), 29829-29837. DOI: 10.1021/acs.jpcc.9b07633.

Zatsepin, Anatoly F; Buntov, Evgeny A; Zatsepin, Dmitry A; Kurmaev, Ernst Z; Pustovarov, Vladimir A et al. (2019). Energy band gaps and excited states in Si QD/SiO x /R yO z (R = Si, Al, Zr) suboxide superlattices. Journal of Physics Condensed Matter 31(41), 415301. DOI: 10.1088/1361-648x/ab30d6.

Zhang, Birong; Kiefer, James R.; Blake, Robert A.; Chang, Jae H.; Hartman, Steven et al. (2019). Unexpected equivalent potency of a constrained chromene enantiomeric pair rationalized by co-crystal structures in complex with estrogen receptor alpha. Bioorganic and Medicinal Chemistry Letters 29(7). DOI: 10.1016/j.bmcl.2019.01.036. [PDB: 6dfn]

Zhang, Chunzi; Wang, Jian; Li, Yuanshi; Li, Xiaoju; Koughia, Cyril et al. (2019). VO_2 microrods synthesized from V_2O_5 thin films. Applied Surface Science 476, 259-264. DOI: 10.1016/j.apsusc.2019.01.087.

Zhang, Gaixia; Yang, Xiaohua; Dubois, Marc; Herraiz, Michael; Chenitz, Régis et al. (2019). Non-PGM electrocatalysts for PEM fuel cells: effect of fluorination on the activity and stability of a highly active NC_Ar + NH_3 catalyst. Energy and Environmental Sciences 12(10), 3015-3037. DOI: 10.1039/c9ee00867e.

Zhang, Peng; Chen, You-Peng; Qiu, Ju-Hui; Dai, You-Zhi; Feng, Bo et al. (2019). Imaging the Microprocesses in Biofilm Matrices. Trends in Biotechnology 37(2), 214-226. DOI: 10.1016/j.tibtech.2018.07.006.

Zhang, Weijie; Dynes, James J.; Hu, Yongfeng; Jiang, Pingping; Ma, Shengqian et al. (2019). Porous metal-metalloporphyrin gel as catalytic binding pocket for highly efficient synergistic catalysis. Nature Communications 10(1). DOI: 10.1038/s41467-019-09881-9.

Zhang, Weiwei; Melo, Lis G. de A.; Hitchcock, Adam P.; Bassim, Nabil (2019). Electron beam damage of epoxy resin films studied by scanning transmission X-ray spectromicroscopy. Micron 120, 74-79. DOI: 10.1016/j.micron.2019.02.003.

Zhang, Haiping; Lin, Hongfei; Zheng et al. (2019). Deactivation mechanism study of unsupported nano MoS_2 catalyst. Carbon Resources Conversion. DOI: 10.1016/j.crcon.2019.09.003.

Zhang, Honglin; Belev, George; Stewart et al. (2019). Protocol development for synchrotron contrast-enhanced CT of human hip cartilage. Medical Engineering Physics 73, 1-8. DOI: 10.1016/j.medengphy.2019.08.003.

Zhang, Longsheng; Wang, Liping; Lin et al. (2019). A Lattice-Oxygen-Involved Reaction Pathway to Boost Urea Oxidation. Angewandte Chemie - International Edition 58(47), 16820-16825. DOI: 10.1002/anie.201909832.

Zhao, Jinxian; Shi, Ruina; Quan et al. (2019). Highly efficient synthesis of dimethyl carbonate over copper catalysts supported on resin-derived carbon microspheres. Chemical Engineering Science 207, 1060-1071. DOI: 10.1016/j.ces.2019.07.039.

Zheng, Tingting; Jiang, Kun; Ta, Na; Hu, Yongfeng; Zeng, Jie et al. (2019). Large-Scale and Highly Selective CO_2 Electrocatalytic Reduction on Nickel Single-Atom Catalyst. Joule 3(1), 265-278. DOI: 10.1016/j.joule.2018.10.015.

Zhou, Laidong; Assoud, Abdeljalil; Zhang, Qiang; Wu, Xiaohan; Nazar, Linda F. et al. (2019). New Family of Argyrodite Thioantimonate Lithium Superionic Conductors. Journal of the American Chemical Society 141(48), 19002-19013. DOI: 10.1021/jacs.9b08357.

Zou, Chengqin; Xi, Cong; Wu, Deyao; Mao, Jing; Liu, Min et al. (2019). Porous Copper Microspheres for Selective Production of Multicarbon Fuels via CO_2 Electroreduction. Small, 1902582. DOI: 10.1002/smll.201902582.

Zou, Yihui; Zhang, Wei; Chen, Ning; Chen, Shuai; Xu, Wenjia et al. (2019). Generating Oxygen Vacancies in MnO Hexagonal Sheets for Ultralong Life Lithium Storage with High Capacity. ACS Nano. DOI: 10.1021/acsnano.8b08608.

von Gunten, Konstantin; Bishop, Brendan; Plata Enriquez, Isabel; Alam, Md. Samrat; Blanchard, Peter et al. (2019). Colloidal transport mechanisms and sequestration of U, Ni, and As in meromictic mine pit lakes. Geochimica et Cosmochimica Acta 265, 292-312. DOI: 10.1016/j.gca.2019.09.015.

DOCTORAL THESIS

Arthur; Zachary (2019). In situ synchrotron radiation investigation of charge compensation and phase evolution mechanisms in Li_2FeSiO_4 electrodes. Supervisor: Jiang, De-Tong. Ontario, Canada: University of Guelph. http://hdl.handle.net/10214/16086.

De Luna; Phil (2019). Nanostructured Electrocatalysts for CO2 Conversion. Supervisor: Sargent, Edward H. ON, Canada: University of Toronto. http://hdl.handle.net/1807/95774.

Fraund; Matthew W. (2019). Developing X-ray Spectromicroscopic Techniques to Quantitatively Determine Population Statistics and Individual Particle Composition of Complex Mixed Aerosols. Supervisor: Moffet, Ryan C. California, USA: University of the Pacific. https://scholarlycommons.pacific.edu/uop_etds/3622/.

Heberlig; Graham William (2019). Harnessing Natural Product Biosynthesis to Access Macrocycles. Supervisor: Boddy, Christopher. Ontario, Canada: University of Ottawa. http://hdl.handle.net/10393/39260..

Lambrecht; Nicholas (2019). Insights into Early Earth Ocean Biogeochemistry from Intensive Monitoring of Two Ferruginous Meromictic Lakes. Supervisor: Swanner, Elizabeth D. Iowa, US: Iowa State University. https://lib.dr.iastate.edu/etd/17493/

Kolaceke, Anezka Popovski (2019). Applications of synchrotron radiation techniques to the study of taphonomic alterations and preservation in fossils. Supervisor: Barbi, Mauricio; McKellar, Ryan. SK, Canada: University of Regina. https://ourspace.uregina.ca/handle/10294/8838.

Li, Tang (2019). Structure-biological function study of 17B-hydroxysteroid dehydrogenase type 1 and reductive steroid enzymes: inhibitor design targeting estrogen-dependent diseases. Supervisor: Lin, Sheng-Xiang. Quebec, Canada: Université Laval. http://hdl.handle.net/20.500.11794/34398.

Li, Zhejun (2019). Materials Design and Mechanistic Investigation of High-Energy-Density Sulfur-Based Batteries. Supervisor: Lu, Yi-Chun. Hong Kong,China: The Chinese University of Hong Kong (Hong Kong). https://search.proquest.com/docview/2310307881.

Longfei Wu (2019). Transition metal chalcogenide based functional materials for renewable energy conversion. Supervisor: Hensen, Emiel, Hofmann, Jan Philipp. Eindhoven, the Netherlands: Technische Universiteit Eindhoven. https://research.tue.nl/en/publications/transition-metal-chalcogenide-based-functional-materials-for-rene.

Mallette, Evan (2019). Structural and functional characterization of the aminoacetone utilization microcompartment from Mycobacterium smegmatis MC2 155. Supervisor: Kimber, Matthew. Ontario, Canada: University of Guelph. http://hdl.handle.net/10214/16112.

Mazhar, Waqas (2019). 60 GHz Substrate Integrated Waveguide Fed Monolithic Grid Dielectric Resonator Antenna Arrays. Supervisor: Dr. D. Klymyshyn. Saskatoon, Canada: University of Saskatchewan.

Popovoski Kolaceke; Anezka (2019). Applications of Synchrotron Radiation Techniques To The Study Of Taphonomic Alterations and Preservation in Fossils. Supervisor: Barbi, Mauricio; McKellar, Ryan. Saskatchewan, Canada: University of Regina. http://hdl.handle.net/10294/8838.

Rozario, Hoimonti Immaculata (2019). High-Resolution Spectroscopic Studies of Atmospheric Gases. Supervisor: Billinghurst, Brant; Staenz, Karl. Alberta, Canada: University of Lethbridge. https://hdl.handle.net/10133/5413.

Sahan Daksitha Perera (2019). Systematic Investigation of Intermolecular Interactions in NEXAFS Spectroscopy. Supervisor: Urquhart, Stephen. Saskatoon, Canada: University of Saskatchewan. https://harvest.usask.ca/handle/10388/12050.

Sowers; Tyler Dale (2019). Organo-Mineral Associations and Sequestration Mechanisms Impacting Carbon Cycling in Diverse Terrestrial and Aquatic Systems. Supervisor: Sparks, Donald L. DE, USA: University of Delaware. http://udspace.udel.edu/handle/19716/24969.

Vance; Tyler D. R. (2019). Adhesion Proteins: Keeping Bacteria in Their Place. Supervisor: Davies, Peter L. ON, Canada: Queen's University. http://hdl.handle.net/1974/26397.

Von Gunten; Konstantin (2019). Biogeochemistry of meromictic pit lakes and permeable reactive barriers at the Cluff Lake uranium mine. Supervisor: Alessi, Daniel; Konhauser, Kurt. AB, Canada: University of Alberta. https://era.library.ualberta.ca/items/0f84e92f-6479-4b97-8f3b-e20151f67abb.

Voth; Kevin Andrew (2019). Structural Biology of Legionella pneumophila Effectors. Supervisor: Cygler, Miroslaw. SK, Canada: University of Saskatchewan. http://hdl.handle.net/10388/12302.

Wang; Qiong (2019). Corrosion associated failure mechanisms of CoCrMo alloys in total hip replacements. Supervisor: Wang, Rizhi. BC, Canada: University of British Columbia. http://hdl.handle.net/2429/69424

Weeks, Joseph J. (2019). Improving environmental health: Investigations into soil lead and phosphorus fate and transport. Supervisor: Hettiarachchi, Ganga M. Kansas, USA: KANSAS STATE UNIVERSITY. https://krex.k-state.edu/dspace/handle/2097/39683

Xiong; ZiJian (2019). Structural Investigations of Saposin/Hydrolase Systems. Supervisor: Privé, Gilbert. Ontario, Canada: University of Toronto. http://hdl.handle.net/1807/97049.

MASTERS' THESIS

Balakrishnan, Manojkumar (2019). Tailored Electrospun Gas Diffusion Layers for Polymer Electrolyte Membrane Fuel Cells: Design and Durability. Supervisor: Bazylak, Aimy. Ontario, Canada: University of Toronto. http://hdl.handle.net/1807/97839.

Bamrah, Ramandeep Kaur (2019). Evaluation of X-ray Fluorescence Spectroscopy as a Tool for Element Analysis in Pea Seeds. Supervisor: Warkentin, Tom. Saskatchewan, Canada: University of Saskatchewan. https://harvest.usask.ca/handle/10388/11836.

Bruder, Lisza M. (2019). Substrate Specificity of Protein Tyrosine Phosphatase-like myo-Inositol Phosphatases: PhyA in Complex with Ins(1,2,4,5,6)P5, Ins(1,3,4,5)P4, and Ins(1,4,5)P3. Supervisor: Mosimann, Steven C. Alberta, Canada: University of Lethbridge. https://hdl.handle.net/10133/5394.

Bulmer, David Roy (2019). Chemical interactions of citrate, calcium and phosphate in a calcareous Saskatchewan subsoil. Supervisor: Peak, Derek. SK, Canada: University of Saskatchewan. http://hdl.handle.net/10388/11871.

Cavalca Cardoso, Natalia (2019). Development of Synchrotron Based Imaging Tools for Benign Prostatic Hyperplasia Using an Induced Canine Model. Supervisor: Snead, Elisabeth; Pettitt, Murray; Singh, Jaswant. Saskatchewan, Canada: University of Saskatchewan. https://harvest.usask.ca/handle/10388/12354.

Conroy; Brigid (2019). Investigating the physiological function of a Staphylococcus aureus Ntn-hydrolase. Supervisor: Murphy, Michael. BC, Canada: University of British Columbia. http://hdl.handle.net/2429/70578.

Donato, Giovanni (2019). Development of glass-ceramic composites by one-step synthesis methods. Supervisor: Grosvenor, Andrew. SK, Canada: University of Saskatoon. https://harvest.usask.ca/handle/10388/12478

Rasouli, Ashkan (2019). An integrated continuous micro-fluidic switch valve. Supervisor: Zhang, Chris. Saskatchewan, Canada: University of Saskatchewan. https://harvest.usask.ca/handle/10388/11920.

Weeks, Joseph J. (2019). Improving Environmental Health: Investigations Into Soil Lead and Phosphorus Fate and Transport. Supervisor: Hettiarachchi, Ganga M. Kansas, USA: Kansas State University. https://krex.k-state.edu/dspace/handle/2097/39683.

White,Brandy R. (2019). Humanization of a MUC16-Specific Monoclonal Antibody and Characterization of the MUC16 Epitope. Supervisor: Brooks, Cory L. California, United States: California State University, Fresno. http://hdl.handle.net/10211.3/211170.

Zhang, Weiwei (2019). Characterization and simulation of electron/ion beam damage on soft materials in FIB-SEM microscopes. Supervisor: Bassim, Nabil D. Ontario, Canada: McMaster University. http://hdl.handle.net/11375/24341.

PATENT

Cathleen M. Crudden; J. Hugh Horton; Mina Raafat Ryad Narouz; Phillip Unsworth; Zhijun Li et al. (2019). Methods of Forming Carbene-Functionalized Composite Materials. Patent Number: US20190169132A1.

BOOK CHAPTER

Boughner, Julia C.; Cooper; David M.L. (2019). Silver-Albumin Tissue Staining Protocol to Visualize Odontogenesis in Whole Embryos. In Petros Papagerakis(Ed.), Odontogenesis: Methods and Protocols. Humana Press, 197-210 9781493990115.

PROTEIN DATA BANK DEPOSITION

Antoshchenko, T.; Chen, Y.; Hughes et al. (2019). Crystal structure of ATPase domain of Human GRP78 bound to Ver155008. Protein Data Bank: 6cz1.

Bamford, N.C.; Subramanian, A.S.; Millan et al. (2019). Crystal Structure of Aspergillus fumigatus Ega3. Protein Data Bank: 6oj1.

Brooks, C.L. (2019). Structure of VHH R419 isolated from a pre-immune phage display library. Protein Data Bank: 6dyx.

Caveney, N.A.; Strynadka, N.C.J. (2019). Crystal structure of GIL01 gp7. Protein Data Bank: 6n7o.

Caveney, N.A.; Strynadka, N.C.J.; Caballero et al. (2019). Crystal structure of E. coli PBP5-meropenem. Protein Data Bank: 6ntz.

Doyle, L.; Mallette, E.; Kimber et al. (2019). Escherichia coli KpsC, N-terminal domain. Protein Data Bank: 6mgc.

Doyle, L.; Mallette, E.; Kimber et al. (2019). Thermosulfurimonas dismutans KpsC, beta Kdo 2,4 transferase. Protein Data Bank: 6mgb.

Doyle, L.; Mallette, E.; Kimber et al. (2019). Thermosulfurimonas dismutans KpsC, beta Kdo 2,4 transferase. Protein Data Bank: 6mgd.

Du, Y.L.; Higgins, M.A.; Zhao et al. (2019). N-demethylindolmycin synthase (PluN2) in complex with N-demethylindolmycin. Protein Data Bank: 6p29.

Edwards, T.E.; Abendroth, J.; Safford et al. (2019). Crystal structure of KIT1 in complex with DP2976 via co-crystallization. Protein Data Bank: 6mob.

Evans, S.V.; Haji-Ghassemi, O. (2019). Unliganded S25-5 Fab. Protein Data Bank: 6c5i.

Evans, S.V.; Haji-Ghassemi, O. (2019). S25-5 Fab in complex with Chlamydiaceae-specific LPS antigen. Protein Data Bank: 6c5h.

Fenalti, G. (2019). Crystal structure of the human TTK in complex with an inhibitor. Protein Data Bank: 6n6o.

Fischmann, T.O. (2019). Murine PI3K delta kinsae domain - cpd 1. Protein Data Bank: 6mul.

Garside, E.L.; MacMillan, A.M. (2019). Prp8 RH domain from C. merolae. Protein Data Bank: 6nqi.

Guarne, A.; Almawi, A.W. (2019). Crystal structure of the Escherichia coli sliding clamp-MutL complex.. Protein Data Bank: 6e8e.

Guarne, A.; Almawi, A.W. (2019). Crystal structure of the Bacillus subtilis sliding clamp-MutL complex.. Protein Data Bank: 6e8d.

Gytz, H.; Liang; J.; Liang et al. (2019). mouse beta-mannosidase bound to beta-D-mannose (MANBA). Protein Data Bank: 6ddu.

Gytz, H.; Liang; J.; Liang et al. (2019). mouse beta-mannosidase (MANBA). Protein Data Bank: 6ddt.

Haji-Ghassemi, O.; Evans, S.V. (2019). S25-23 Fab in complex with Chlamydiaceae LPS (Crystal form 2). Protein Data Bank: 6c5k.

Haji-Ghassemi, O.; Evans, S.V. (2019). S25-23 Fab in complex with Chlamydiaceae LPS (Crystal form 1). Protein Data Bank: 6c5j.

Halgas, O.; Zarabi, S.F.; Schimmer et al. (2019). Human mitochondrial ClpP in complex with ONC201 (TIC10). Protein Data Bank: 6dl7.

Huang, J.; Fraser, M.E. (2019). ADP bound to L227bF mutant ATP-grasp fold of Blastocystis hominis succinyl-CoA synthetase. Protein Data Bank: 6no4.

Huang, J.; Fraser, M.E. (2019). ADP bound to V113bL mutant ATP-grasp fold of Blastocystis hominis succinyl-CoA synthetase. Protein Data Bank: 6no3.

Huang, J.; Fraser, M.E. (2019). ADP bound to K114bD mutant ATP-grasp fold of Blastocystis hominis succinyl-CoA synthetase. Protein Data Bank: 6no2.

Huang, J.; Fraser, M.E. (2019). ADP bound to K46bE mutant ATP-grasp fold of Blastocystis hominis succinyl-CoA synthetase. Protein Data Bank: 6no1.

Khan, J.A. (2019). Crystal structure of tyrosine kinase 2 jh2 (pseudo kinase domain) complexed with Compound. Protein Data Bank: 6nzr.

Khan, J.A. (2019). Crystal structure of tyrosine kinase 2 jh2 (pseudo kinase domain) complexed with Compound. Protein Data Bank: 6nzq.

Kiefer, J.R.; Vinogradova, M.; Liang et al. (2019). Crystal structure of estrogen receptor alpha in complex with receptor degrader 16aa. Protein Data Bank: 6dfn.

Kimber, M.S.; Mallette, E.; Aggett et al. (2019). Ltp2-ChsH2(DUF35) aldolase. Protein Data Bank: 6ok1.

Kolesnikov, M.; Murphy, M.E.P. (2019). Crystal structure of Fusobacterium nucleatum flavodoxin mutant K13G bound to flavin mononucleotide. Protein Data Bank: 6ohk.

Kuatsjah, E.; Verstraete, M.M.; Kobylarz et al. (2019). Crystal structure of Sphingomonas paucimobilis TMY1009 LsdA phenylazophenol complex. Protein Data Bank: 6ojt.

Lang, D.E.; Morris, J.S.; Rowley et al. (2019). Tetrahydroprotoberberine N-methyltransferase in complex with S-adenosylhomocysteine. Protein Data Bank: 6p3m.

Langelier, M.F.; Pascal, J.M. (2019). Crystal Structure of human PARP-1 ART domain bound to inhibitor UTT93. Protein Data Bank: 6nrj.

Langelier, M.F.; Pascal, J.M. (2019). Crystal Structure of human PARP-1 ART domain bound to inhibitor UTT83. Protein Data Bank: 6nri.

Langelier, M.F.; Pascal, J.M. (2019). Crystal Structure of human PARP-1 ART domain bound inhibitor UTT63. Protein Data Bank: 6nrh.

Langelier, M.F.; Pascal, J.M. (2019). Crystal Structure of human PARP-1 ART domain bound to inhibitor UTT57. Protein Data Bank: 6nrg.

Langelier, M.F.; Pascal, J.M. (2019). Crystal Structure of human PARP-1 ART domain bound to inhibitor UTT103. Protein Data Bank: 6nrf.

Lei, M.; Tempel, W.; Arrowsmith et al. (2019). MeCP2 MBD in complex with DNA. Protein Data Bank: 6ogj.

Li, T.; Lin, S.X. (2019). Crystal structure of human 17beta-hydroxysteroid dehydrogenase type 1 complexed with estrone and NADP+. Protein Data Bank: 6mne.

Mark, B.L.; Vadlamani, G. (2019). Carbapenemase VCC-1 from Vibrio cholerae N14-02106. Protein Data Bank: 6mk6.

Moore, S.A.; Marshall, J.D.; Anderson et al. (2019). Structure of the Bovine p85a BH domain R228E mutant. Protein Data Bank: 6mrp.

Moore; S.A.; Xiao; W.; Li et al. (2019). Yeast Ddi2 Cyanamide Hydratase. Protein Data Bank: 6dkd.

Moore; S.A.; Xiao; W.; Li et al. (2019). Yeast Ddi2 Cyanamide Hydratase, T157V mutant, apo structure. Protein Data Bank: 6dkc.

Moore; S.A.; Xiao; W.; Li et al. (2019). Yeast Ddi2 Cyanamide Hydratase. Protein Data Bank: 6dka.

Moore; S.A.; Xiao; W.; Li et al. (2019). Yeast Ddi2 Cyanamide Hydratase. Protein Data Bank: 6dk9.

Moss; D.L.; Park; H.W.; Mettu et al. (2019). Pseudomonas exotoxin A domain III T18H477L. Protein Data Bank: 6edg.

Nation; C.; Pizarro; J.C. (2019). Candida albicans Hsp90 nucleotide binding domain in complex with radicicol. Protein Data Bank: 6cjp.

Nation; C.; Pizarro; J.C. (2019). Candida albicans Hsp90 nucleotide binding domain in complex with radicicol. Protein Data Bank: 6cjl.

O'Neill; D. (2019). CRYSTAL STRUCTURE OF SESTRIN2 IN COMPLEX WITH NV-0005138. Protein Data Bank: 6n0m.

Perez-Borrajero; C.; Okon; M.; Lin et al. (2019). ETS1 in complex with synthetic SRR mimic. Protein Data Bank: 6da1.

Pluvinage; B.; Boraston; A.B. (2019). Crystal structure of SpGH29. Protein Data Bank: 6or4.

Raman; S.; Beilschmidt; M.; Fransson et al. (2019). Crystal structure of Frizzled 7 CRD in complex with F7.B Fab. Protein Data Bank: 6o3a.

Raman; S.; Beilschmidt; M.; Fransson et al. (2019). Crystal structure of Frizzled 5 CRD in complex with F2.I Fab. Protein Data Bank: 6o39.

Ryan; P.; Kimber; M.S. (2019). RbcS-like subdomain of CcmM. Protein Data Bank: 6mr1.

Sack; J. (2019). Crystal structure of RAR-related orphan receptor C (NHIS-RORGT(244-487)-L6-SRC1(678-692)) in complex with a phenyl (3-phenylpyrrolidin-3-yl)sulfone inhibitor. Protein Data Bank: 6p9f.

Sack; J.S. (2019). Crystal structure of JAK3 kinase domain in complex with a pyrrolopyridazine carboxamide inhibitor. Protein Data Bank: 6ny4.

Sahtout; N.; Kuttiyatveetil; J.R.; Sanders et al. (2019). Structure of thioredoxin 1 from the thermophilic eubacterium Thermosipho africanus TCF52B. Protein Data Bank: 6mos.

Shah; M.; Thavalingham; A.; Maxwell et al. (2019). Structure of anti-crispr protein, AcrIIC2. Protein Data Bank: 6n05.

Shi; R. (2019). Crystal structure of the dimeric bH1-Fab variant [HC-Y33W,HC-D98F,HC-G99M,LC-S30bR]. Protein Data Bank: 6my5.

Shi; R. (2019). Crystal structure of the dimeric bH1-Fab variant [HC-Y33W,HC-D98M,HC-G99M]. Protein Data Bank: 6mxr.

Shi; R.; Picard; M.-E.; Manenda et al. (2019). Crystal structure of the dimeric bH1-Fab variant [HC-Y33W,HC-D98M,HC-G99M,LC-S30bR]. Protein Data Bank: 6my4.

Shi; R.; Picard; M.-E.; Manenda et al. (2019). Crystal structure of the dimeric bH1-Fab variant [HC-Y33W,HC-D98F,HC-G99M]. Protein Data Bank: 6mxs.

Sim; L.; Rahfeld; P.; Withers et al. (2019). Crystal structure of an N-acetylgalactosamine deacetylase from F. plautii in complex with blood group B trisaccharide. Protein Data Bank: 6n1b.

Sim; L.; Rahfeld; P.; Withers et al. (2019). Crystal structure of an N-acetylgalactosamine deacetylase from F. plautii. Protein Data Bank: 6n1a.

Simonetta; K.R.; Clifton; M.C.; Walter et al. (2019). Monophosphorylated pSer33 b-Catenin peptide bound to b-TrCP/Skp1 Complex. Protein Data Bank: 6m94.

Simonetta; K.R.; Clifton; M.C.; Walter et al. (2019). Monophosphorylated pSer33 b-Catenin peptide, b-TrCP/Skp1, NRX-103094 ternary complex. Protein Data Bank: 6m91.

Simonetta; K.R.; Clifton; M.C.; Walter et al. (2019). Monophosphorylated pSer33 b-Catenin peptide, b-TrCP/Skp1, NRX-2663 ternary complex. Protein Data Bank: 6m92.

Simonetta; K.R.; Clifton; M.C.; Walter et al. (2019). Monophosphorylated pSer33 b-Catenin peptide, b-TrCP/Skp1, NRX-1933 ternary complex. Protein Data Bank: 6m93.

Stogios; P.J.; Skarina; T.; Arnal et al. (2019). Crystal structure of Streptomyces rapamycinicus GH74 in complex with xyloglucan fragments XLLG and XXXG. Protein Data Bank: 6p2o.

Stogios; P.J.; Skarina; T.; Arnal et al. (2019). Crystal structure of Niastella koreensis GH74 (NkGH74) enzyme. Protein Data Bank: 6p2l.

Stogios; P.J.; Skarina; T.; Arnal et al. (2019). Crystal structure of the catalytic domain from GH74 enzyme PoGH74 from Paenibacillus odorifer, D60A mutant in complex with XXLG and XGXXLG xyloglucan. Protein Data Bank: 6mgl.

Suits; M.D.L.; Whiteside; J. (2019). PntC-AEPT: fusion protein of phosphonate-specific cytidylyltransferase and 2-aminoethylphosphonate (AEP) transaminase from Treponema denticola in complex with cytidine monophosphate-AEP. Protein Data Bank: 6pd2.

Tamura; K.; Gardill; B.R.; Brumer et al. (2019). Bacteroides ovatus mixed-linkage glucan utilization locus (MLGUL) SGBP-B in complex with mixed-linkage heptasaccharide. Protein Data Bank: 6e9b.

Wei; Y.; Prive; G.G. (2019). Crystal structure of deglycosylated human EPDR1. Protein Data Bank: 6e7o.

Xu; C.; Boniecki; M.; Cygler et al. (2019). Structure of the N-terminal domain of effector protein SpvB from Salmonella typhimurium strain LT2. Protein Data Bank: 6p0x.

Yachnin; B.J.; Berghuis; A.M. (2019). Crystal structure of trimethoprim-resistant type II dihydrofolate reductase in complex with a bisbenzimidazole inhibitor. Protein Data Bank: 6ny0.

Yu; C.; Drobnick; J.; Bryan et al. (2019). Structure of the IRAK4 kinase domain with compound 5. Protein Data Bank: 6o9d.

van Petegem; F.; Haji-Ghassemi; O. (2019). Catalytic subunit of cAMP-dependent protein kinase A in complex with RyR2 K2879A, S2813D phosphomimetic (2699-2904) crystal form 1. Protein Data Bank: 6mm7.

van Petegem; F.; Haji-Ghassemi; O. (2019). Catalytic subunit of cAMP-dependent protein kinase A in complex with RyR2 phosphorylation domain (2699-2904). Protein Data Bank: 6mm6.

ACRONYM GLOSSARY

BEAMLINES

BioXAS: Biological X-ray Absorption Spectroscopy

BMIT: Biomedical Imaging and Therapy

BXDS: Brockhouse X-Ray Diffraction and Scattering Sector

CLS@APS: CLS at the Advanced Photon Source

CMCF: Canadian Macromolecular Crystallography Facility

Far-IR: Far Infrared Spectroscopy

HXMA: Hard X-ray MicroAnalysis

IDEAS: Industry Development Education Applications Students

Mid-IR: Mid Infrared Spectromicroscopy

REIXS: Resonant Elastic and Inelastic X-ray Scattering

SGM: High Resolution Spherical Grating Monochromator

SM: Soft X-ray Spectromicroscopy

SXRMB: Soft X-ray Microcharacterization Beamline

SyLMAND: Synchrotron Laboratory for Micro And Nano Devices

VESPERS: Very Sensitive Elemental and Structural Probe Employing Radiation from a Synchrotron

VLS-PGM: Variable Line Spacing Plane Grating Monochromator

QMSC: Quantum Materials Spectroscopy Center